Environmental Earth Sciences (2023) 82:515
https://doi.org/10.1007/s12665-023-11202-9

ORIGINAL ARTICLE

Geochemical dynamics of phosphorus and metals in sediments of a shallow coastal lake (Xuño Lake, Galicia-NW Iberian Peninsula)

X. L. Otero[1,2] · P. Fraga[1] · A. Merino[3] · R. Carballeira[4]

Received: 26 February 2023 / Accepted: 18 September 2023 / Published online: 7 October 2023
© The Author(s) 2023

Abstract

The shallow lakes are important freshwater ecosystems, since they support much of biodiversity and ecosystem services of life on land. Shallow lakes are highly dynamic ecological entities that can exist in several alternative stable states through regime shift caused by a natural or human disturbance that exceeds ecological thresholds for biological communities composition and structure equilibria. The sediment as a reservoir has a key role in the limnological regulation of wetlands linked to the fluxes of nutrients and elements in the biogeochemical interplay with the water and macrophytes. For this reason, the role of sediment in the limnology of the shallow coastal lake of Xuño (NW Iberian Peninsula) was explored by seasonally monitoring the chemical composition of water and sediments, also according to macrophyte species. The shallow depth determines the high availability of light in the bottom and a well-mixed water column maintain the surface of the water–sediment interface oxygenated. The oxic conditions of the bottom implies a top-down regulation of the water column in the Xuño shallow lake that limits the diffusion of phosphorus and trace metals (Fe, Mn, Cu, and Co) to the water, buffering eutrophication or contamination levels by immobilization in the sediments. In fact, the concentration of Hg in the lake water in spring, and also its bioavailability, are high due to its release from the sediment in suboxic conditions. The cover of helophyte species *Phragmites Australis* and *Schoenoplectus Lacustris* showed differences in the assimilation of organic monoester and diester phosphorus forms in the sediment. However, the water of the Xuño Lake shows an eutrophic status by the nutrient input associated with the birds populations as indicated by microbiological data.

Keywords Geochemistry · Limnology · Ecological trophic status · Macrophytes · Eutrophication · Metal contamination

Introduction

Shallow lakes are very dynamic ecosystems that can change from one ecological status to another if an impact is greater than the ecosystem's resilience thresholds (Jeppesen et al. 1997; Moss et al. 1997; Scheffer and van Nees 2007). The depth of shallow lakes allows light to reach the bottom throughout the year, leading to high nutrient recycling rates in the water column, mainly of phosphorus, which is the limiting element in freshwater wetlands. This implies an interplay between phytoplankton in the water column and bottom-rooted macrophytes bound to the sediment, which determines the ecological structure of the lake ecosystem, so that it can recruit a high biodiversity in its optimal ecological state (Jeppesen et al. 1997).

In addition, the shallow depth implies a water volume to sediment surface area high ratio, which may play an important role in top-down or bottom-up regulation of the limnology of shallow lakes (Vadeboncoeur et al. 2001;

✉ R. Carballeira
rafael.carballeira@uv.es; rafael.carballeira@gmail.com

X. L. Otero
xl.otero@usc.es

1 CRETUS, Departamento de Edafoloxía e Química Agrícola, Facultade de Bioloxía, Universidade de Santiago de Compostela, 15782 Santiago, Spain

2 REBUSC, Rede das Estacións Biolóxicas da Universidade de Santiago de Compostela, Universidade de Santiago de Compostela, 15782 Santiago, Spain

3 Departamento de Edafoloxía e Química Agrícola, Escola Politécnica de Superior de Lugo, Universidade de Santiago de Compostela, 27002 Lugo, Spain

4 Cavanilles Institute for Biodiversity and Evolutionary Biology, University of Valencia, 46980 Paterna, Valencia, Spain

Søndergaard et al. 2003; Janse et al. 2008; Harrault et al. 2014). The regime shift of freshwater aquatic ecosystems is highly dependent on the bioavailability of phosphorus in the water column, although phosphorus levels are modulated by the interaction with iron and sequestered in the sediment depending on environmental conditions (Gebremariam et al. 2021; Li et al. 2021). Sediments are a reservoir of nutrients, metals, and other elements that are several orders of magnitude higher than in the water column; thus, a small alteration of the equilibrium of the sediment–water interface can lead to drastic geochemical changes in water composition, greatly impacting the structure of biological communities (Hupfer and Dollan 2003; Kim et al. 2003; Nowlin et al. 2005; Zhu et al. 2013). In addition, metal bioavailability has important repercussions at the level of the entire food web (Janssen et al. 2021).

Shallow lakes are highly productive ecosystems that support a major aquatic and terrestrial biodiversity, even despite the small dimensions of some lakes, but they maintain a fragile balance that can be altered by an increase in nutrients leading to a regime shift, with a high loss of biodiversity and deterioration of ecosystem services (Declerck et al. 2005). Shallow wetlands are especially important in bird conservation because of their crucial role in supporting waterbirds populations and biodiversity, or as favourable migration or breeding habitat for many bird species (Kleijn et al. 2014; Zhang et al. 2015; Gaget et al. 2020), although the influence of birds on the trophic status of shallow wetlands is still widely unknown (Dejoux 1983; Gere and Andrikovics 1992; Suter 1994; Hansson et al. 2010).

Currently, global change entails an alteration in the climatic parameters that affect hydrological regimes and temperatures in wetlands worldwide (Foley et al. 2012; Jeppesen et al. 2014; Yankova et al. 2017; Maberly et al. 2020; Woolway et al. 2021). Therefore, unravelling the complex abiotic and biotic interactions that regulate biogeochemical cycling of nutrients and metals in the different geochemical compartments of lake ecosystems is a major challenge, especially due to the spatial heterogeneity in the distribution of macrophytes and the large seasonal fluctuations in the chemical conditions of the water column. For this reason, the role of sediment in the complex regulation of nutrients and metal mobility in freshwater aquatic ecosystems has been studied by monitoring an unpolluted shallow coastal lake in Galicia (NW Iberian Peninsula).

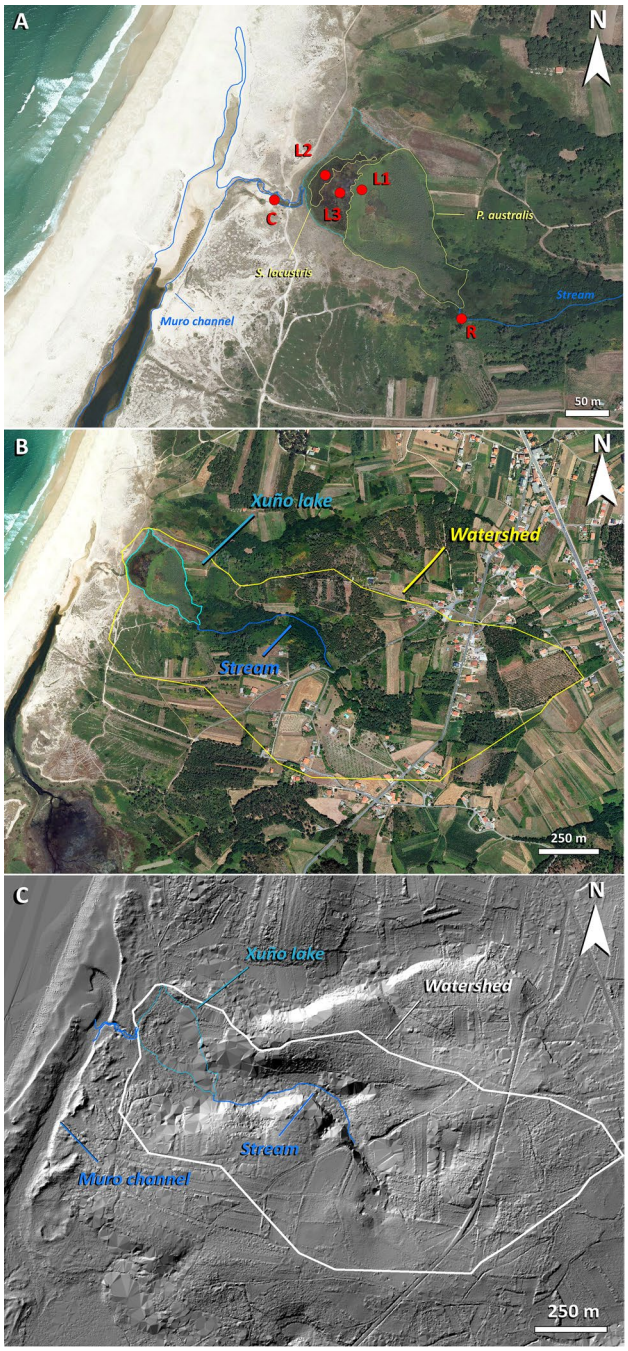


Fig. 1 Location of the Xuño shallow coastal lake (Galicia, NW Iberian Peninsula): **a** Detail of the lake, the areas dominated by helophytes and the sampling points: L1—area dominated by *P. australis*, L2—area dominated by *S. lacustris*, L3—open water area, R—stream, and C—lake channel; **b**, **c** area of the Xuño Lake hydrological basin, **b** aerial orthophoto (PNOA 2010) and **c** terrain elevation model (LiDAR 2008–2015) (Spanish National Center for Geographic Information (CNIG): https://www.ign.es/web/gl/qsm-cnig)

Study area

Xuño Lake is located in the town of Porto do Son (A Coruña, Galicia) (UTM 29 T 496856 X, 4,720,099 Y; Datum ETRS89) in the NW Iberian Peninsula (Fig. 1). It is a shallow freshwater coastal lake with an area of 2.67 ha and a maximum depth of 2 m. The lake is fed by a 478.6 m-long freshwater stream and experiences a severe drop in water levels during the summer, even drying out

completely in some years depending on seasonal rainfall. Xuño Lake is perched atop elevated raised granite promontory at an altitude of 5.5 m a.s.l. closed by the formation of a sand dune; thus, it is a back-barrier perched lake, according to the typology described by Sáez et al. (2018), and it drains through a short stream across the dune into the long channel of the nearby Muro Lagoon. The basin of the lake, with a total area of 52.63 ha, is dominated by of schists and paragneisses, although the lake is located on a small Holocene alluvial plain (IGME1981). Land use comprises a mosaic of suburban areas (5.71%), groups of small agricultural plots (36.27%), forest plantations (*Pinus* spp., *Eucalyptus* spp.) (31.48%), and renaturalized areas (21.47%) around the Xuño Lake (Fig. 1).

Xuño Lake corresponds to Habitat 3130, Oligotrophic to mesotrophic standing waters with vegetation of the *Littorelletea uniflorae,* and 3150 Natural eutrophic lakes with Magnopotamion or Hydrocharition-type vegetation (European Union Habitats Directive 92/43/CEE 1992), and it is included in the Natura 2000 Network, protected by the Corrubedo Wetland Complex Special Area of Conservation ZEC ES1110006 (Decree 37/2014). Its shallow depth allows for the development of macrophytic vegetation across the lake's surface during the summer. The aquatic vegetation is dominated mainly by hydrophytes *Nymphaea alba*, *Potamogeton trichoides,* and *Utricularia australis*, while the shoreline is dominated by helophytes *Phragmites australis, Typha latifolia* and *Schoenoplectus lacustris*; in addition, *Littorella uniflora* is abundant in the shallow edge areas with great seasonal fluctuations in water level.

Materials and methods

Xuño Lake was monitored at five sampling points. Three of these points were located on the lake in the deepest zone according to the different vegetation zones (Fig. 1): two points in areas dominated by helophytes *Phragmites australis* (Cav.) Trin. Ex Steud. (L1) (UTM 29 T 496842 X, 4,720,141 Y; ETRS98) and *Schoenoplectus lacustris* (L.) Pallas (L2) (UTM 29 T 496785 X, 4,720,150 Y; ETRS98) and another point in the open water zone dominated by hydrophytes (L3) (UTM 29 T 496800 X, 4,720,135 Y; ETRS98). The two remaining sampling points were located in the tributary stream that feeds the lake I (UTM 29 T 496952 X, 4,719,955 Y; ETRS98) and in the lake's drainage channel(C) (UTM 29 T 496704 X, 4,720,138 Y; ETRS98). Points were sampled seasonally three times a year (i.e., in the winter, spring, summer–autumn) from autumn 2009 to autumn 2011.

Water analyses

Water chemical analyses

Temperature (ºC), pH, electrical conductivity (E.C.) (µS cm^{-1}), salinity (‰), oxygen saturation percentage (%), and redox potential (Eh) (mV) were measured in situ using a Hanna HI9828 multiparametric probe. Salinity ranges were established according to The Venice System for the Classification of Marine Waters According to Salinity (1959). Water sampling stations for chemical analyses were located at 0.5 m depth in the water column. Water samples were collected with 1 L Teflon bottles and divided into subsamples for the different laboratory analyses; subsamples were stored at 4 °C and avoiding direct sunlight.

Biochemistry Oxygen Demand (BOD5) was measured in the laboratory on the day of collection using an OxiTop Box (WTW). Water samples for nutrient determination (NO_3^-, NO_2^-, NH_4^+, PO_4^{3-}) were stored in 50 mL bottles and frozen at – 20 °C until analysis. In addition, water samples for the determination of dissolved organic carbon (DOC), alkalinity, major anionic ions (SO_4^{2-}, Cl^-), sodium (Na^+) and total suspended solids (TSS) were stored in 150 mL bottles at 4 °C, avoiding direct sunlight. DOC (mg L^{-1})—analyzed using a Systea-Flowsys equipment—alkalinity (meq L^{-1}) and nutrients in water (NO_3^-, NO_2^-, NH_4^+, PO_4^{3-}) (mg L^{-1}) were analyzed using standard colorimetric methods (Hansen and Koroleff 1999). Major anionic ions (SO_4^{2-}, Cl^-) (mg L^{-1}) were analyzed using a Dionex 4500I Ion exchange chromatographer. Sodium was analyzed using a 7900 × Agilent ICP-MS at the University of Santiago de Compostela's research services (Red de Infraestructuras de Apoyo a la Investigación y al Desarrollo Tecnológico; RIAIDT-USC).

Total suspended solids (TSS) (mg L^{-1}) in water were determined by filtering 100 mL in water volume through GF/F filters and calculating the difference in weight between the filters before and after drying at least 1 h at 104 °C.

Water samples were taken in the lake and outlet channel in spring of 2010 for trace metal determination were stored in 50 mL teflon bottles and pre-acidified with 0.02 N nitric acid (pH < 2) at 4 °C and avoiding direct sunlight. Trace metals and metalloids in water (i.e., As, Cd, Co, Cr, Cu, Fe, Hg, Mn, Mo, Na, Ni, Pb, Se and Zn) were analyzed using a 7900 × Agilent ICP-MS at the University of Santiago de Compostela's research services (Red de Infraestructuras de Apoyo a la Investigación y al Desarrollo Tecnológico; RIAIDT-USC).

Measurement precision was assessed by relative standard deviation (RSD), which remained lower than 5%. Detection limits, expressed as three times the standard deviation of 10 replicate measurements of reagent blanks, were 1 mg L^{-1}

for DBO5, 0.01 mg L^{-1} for DOC, 0.04 mg L^{-1} for nitrate, 0.01 mg L^{-1} for nitrite, 0.02 mg L^{-1} for ammonium, 0.02 mg L^{-1} µM for phosphate and 0.01 µg L^{-1} for trace metals.

Water microbiological analyses

Water samples for microbiological analyses were taken at 0.5 m depth in the water column and stored in 2 L sterile bottles at 4 °C, avoiding direct sunlight, until analysis in the laboratory. Water samples were filtered (0.45 µm pore size, 47 mm diameter; Whatman® nylon membrane filters) to quantify total coliforms, fecal coliforms and fecal streptococci over a range of dilutions via standard membrane filtration methods according to the European Union Directive (2006/7/CE).

Sediment analyses

Grain size analysis and chemical analysis

Bottom sediments were taken by extracting cores from lake sampling points L1–L3 using PVC tubes: two cores with a length of 50 cm and a diameter of 10.3 cm were collected at points L1 *P. australis* vegetated and L2 *S. lacustris*, and one core with a length of 110 cm and a diameter of 4.5 cm was collected at open-water point L3 point. The cores were kept tightly closed and in an upright position during transport to the laboratory and subsequently opened in half and sampled at 2.5 cm-thick levels. Samples from each hemicylinder were ground after drying in an oven at ~ 40 ºC for 48 h or storage at – 20 ºC, respectively.

pH and redox potential were determined on wet sediment samples within 24 h of collection using a micro pH 2000 and a GLP31 Crison device, respectively. Total carbon (TC) and sulfur (TS) contents were determined from dry ground sediment samples using a Leco CS144DR combustion elemental analyzer. Grain sizes were determined on a 2 g dry sediment subsample by sieving through 2–0.05 mm mesh sizes for the sandy fraction and < 0.05 mm for the fine fraction (silts and clays), respectively.

Metals

Chemical speciation of metals iron (Fe), manganese (Mn), copper (Cu) and cobalt (Co) was determined by a sequential extraction process according to Otero et al. (2000, 2005, 2009) and Otero and Macías (2003) on 2 g wet sediment samples to avoid disturbance of the reduced forms, a modification from the combination of methodologies by Tessier et al. (1979), Fortin et al. (1993) and Huerta-Díaz and Morse (1990). Metals in the different fractions were measured on the supernatant recovered after chemical attack by serial centrifugation at 1200×*g* for 30 min at 4 ºC (Tessier et al. 1979).

- Metal fraction 1 (F1) is associated with mobile and interchangeable metals. This fraction was extracted from 2 g of wet sediments by adding 30 ml 1 M $MgCl_2$ (pH = 7) and shaking for 30 min (Tessier et al. 1979).
- Metal fraction 2 (F2) is associated with carbonates. This fraction was extracted from the pellet of the previous F1 sample by adding 30 ml 1 M sodium acetate (pH = 5) and shaking for 5 h (Tessier et al. 1979).
- Metal fraction 3 (F3) is associated with iron oxides and hydroxides, both crystalline (i.e., goethite and hematite) and amorphous (i.e., lepidocrocite, ferrihydrite). This fraction was extracted from the pellet of the previous F2 sample by adding a 1:1 dissolution of 20 ml 0.25 M sodium citrate and 11 M sodium bicarbonate with 3 g sodium dithionite and shaking for 30 min at 75 ºC (Fortin et al. 1993).
- Metal fraction 4 (F4) is associated with pyrite. Fe associated with silicates and organic matter were previously removed from the F3 sample pellet by two successive acid treatment steps: (i) the sample was treated with 10 M HF and shaken for 16 h, then treated with H_3BO_3 and shaken for 8 h; (ii) the sample was treated with H_2SO_4 and shaken for 2 h. Finally, F4 was extracted by adding 10 ml of HNO_3 and shaking for 2 h, after which 15 ml of bi-distilled water were added (Otero et al. 2023).

Iron, manganese, copper and cobalt contents of each fraction were determined by spectroscopy, according to Bruland et al. (1979). Fe and Mn were measured using a Perkin Elmer 1100B flame atomic absorption spectrometer. Cu and Co were measured using a Perkin Elmer 4110ZL graphite furnace atomic absorption spectrometer. Detection limits, expressed as three times the standard deviation of 10 replicate measurements of reagent blanks, were 0.03 µmol g^{-1} for Fe, 5 nmol g^{-1} for Mn and 0.1 nmol g^{-1} for Cu and Co.

Phosphorus speciation

Phosphorus adsorbed on Fe–Mn oxides and Al–silica clay oxides was extracted jointly with NaOH (Ann et al. 2000a, 2000b; Schlichting et al. 2002; Hogan et al. 2004), a modification of the original method according to Paludan and Jensen (1995) and Paludan and Morris (1999). The P content in sediment samples, measured as soluble P after chemical extraction of fractions, was analysed using a Helios γ Thermo Spectronic spectrophotometer according to standard colorimetric methods (Hansen and Koroleff 1999). P in the different fractions was measured on the supernatant recovered after subjecting 2 g of wet sediment sample to chemical attack by serial centrifugation at 1200×*g* for 30 min at 4 ºC.

Fraction 1 (F1) is soluble and adsorbed P. A 2 g wet sediment subsample was treated with 20 ml of $MgCl_2$ 1 M and shaken for 1 h.

Fraction 2 (F2) is P adsorbed on Fe oxides and hydroxides. The F1 pellet was treated with a 1:1 dissolution of 20 ml 0.11 M $NaHCO_3$ and 0.11 M $Na_2S_2O_4$ and shaken for 18 h.

Fraction 3 (F3) is P associated with silica clay minerals and Al hydroxides. The F2 pellet was treated with 20 ml 0.1 M NaOH and shaken for 18 h. Fraction 3B (F3B), P associated with humic acids, was extracted to avoid interferences in colorimetric measurements due to solubilization of humic acids in alkaline conditions. A F3 supernatant subsample was treated with 2.5 ml H_2SO_4 for 12 h; the samples were subsequently filtered through an Albert paper and dried in a stove at 45 ºC. Once dry, the paper was cut into pieces, placed in crucibles and calcined at 520 ºC in a muffle for 2 h (Holmboe et al. 2001). F3B was extracted using 10 ml of boiling 1 M HCL (Paludan and Jensen 1995; Paludan and Morris 1999).

Fraction 4 (F4) is P linked to apatite. The F3 pellet was treated with 0.5 M HCl and shaken for 1 h.

Fraction 5 (F5) is P associated with refractory organic matter. The F4 pellet was dried at 45 ºC in an oven. Once dry, the sample was burned in a muffle at 520 ºC for 2 h, and the sample was subsequently transferred to a tube with 10 ml 1 M HCl for 20 min at 100 ºC. Samples were topped up to 100 ml with bi-distilled water. 20-ml aliquots were collected in plastic tubes and stored at 3 ºC in a refrigerator until analysis.

Organic phosphorus

Organic phosphorus was extracted from sediment using NaOH–EDTA (Noack et al. 2012). The organic fraction was extracted from 1 g of wet sediment by adding 30 ml 0.25 M NaOH and 50 mM EDTA and shaking for 16 h. After this treatment, the organic extract was recovered by centrifugation at 900×*g* for 10 min, and 20 ml of the supernatant were transferred to a new tube. Subsequently, 1 ml of 50 mg ml^{-1} methylene diphosphonic acid (MDPA) was added as an internal standard, and the extract was frozen to -80 ºC and freeze-dried until analysis. Organic P speciation was determined by nuclear magnetic resonance (NMR) spectroscopy of ^{31}P (Cade-Menun 2005). 300 mg subsamples from each freeze-dried sample were redissolved in 0.3 ml D_2O and 2.7 ml of a 1:1 dissolution of 0.1 M NaOH and 0.1 M EDTA. The spectra were obtained using a VNMRS-500-WB NMR spectrometer at a frequency of 202.296 MHz and at a temperature of 25 ºC (García-Oliva et al. 2018).

The spectroscopic signals were assigned to the different forms of P according to Turner et al. (2003): orthophosphate (5.3 ppm), orthophosphate monoesters (3–5.1 ppm), pyrophosphate (5.5 ppm) and orthophosphate diester (0–2 ppm). Spectra were processed using the MestreNova 8.1.0 program (Mestrelab Research Inc., Santiago de Compostela, Spain).

Results

Water chemical and microbiological analyses

The main physico-chemical parameters of the water are summarized in Table 1. Freshwater from Xuño Lake did not show any seawater intrusion throughout the year, with a Na/Cl ratio > 0.86, and were found to be poorly mineralized waters with salinity < 0.5‰ and electrical conductivity < 500 µS cm^{-1} (Fig. 2), except for the summer season, when the lack of rain and water inputs from the lake basin led to strong evaporation and even to desiccation, with increased salinity levels within the oligohaline range (< 2‰) and electrical conductivity < 1000 µS cm^{-1}. Major ion concentrations were low (Cl^- 47.0–827.5 mg L^{-1}; SO_4^{2-} 2.25–26.2 mg L^{-1}; Na^+ 29.5–33.4 mg L^{-1}). pH range was circumneutral (5.7–7.4) (Table 1; Fig. 2). Waters of Xuño Lake were well-oxygenated during the rainy season period, as indicated by oxygen concentrations of 4–15 mg L^{-1} and redox potential values (Eh) > 400 mV, and showed a low organic load, as indicated by DBO_5 levels fo 0–19 mg L^{-1} and TOC values < 10 mg L^{-1}, although the low water level and high evaporation rate at the end of summer caused a period of anoxia, with oxygen concentration < 3 mg L^{-1} and redox potential < 250 mV (Table 1). Nutrient levels were low all year round, both for N (NO_3^- < 0.50 mg L^{-1}, NO_2^- < 0.06 mg L^{-1}, NH_4^+ < 0.50 mg L^{-1}) and for P (PO_4^{3-} < 0.050 mg L^{-1}), although nitrates were related to the inflow of runoff water during the rainy season, while reduced nitrogen and phosphates forms were associated with the anoxic period during the summer (Table 1). Moreover, trace metal concentrations in water were very low < 1 µg L^{-1} (Table 1).

The microbiological data of the tributary stream are summarized in Table 2. Values were low for aerobic bacteria, faecal streptococci, and faecal and total coliforms (Royal Decree 817/2015), although an increase was observed in the summer, particularly in total coliforms (> 10^3 UFC 100 mL^{-1}) and total aerobic bacteria (> 10^3 UFC mL^{-1}).

Sediment analysis

Grain size and geochemistry of lacustrine sediments

The granulometry of sediments from Xuño Lake showed a higher percentage of fine particles (clays and silts) in surface levels across the profile, with a drastic increase in sand with depth (> 85–90%). This change occurred at a depth of 12 cm in the zone dominated by *S. lacustris* and at a depth of 30 cm in the *P. australis* zone and the central open-water zone (Fig. 3).

Table 1 Summary of the main parameters of the water of Xuño Lake (2009–2011): a biochemical oxygen demand (BOD_5) (mg l^{-1}), b oxygen concentration (mg l^{-1}), c suspended solids (g l^{-1}), d redox potential (mV), e alkalinity (meq l^{-1}), f dissolved organic carbon (DOC) (mg l^{-1}), g ammonium (mg l^{-1}), h nitrites (mg l^{-1}), i nitrates (mg l^{-1}), j phosphates (mg l^{-1}), k chlorides (mg l^{-1}), l sulfides (mg l^{-1}), m trace metals in water (μg l^{-1}) (As, Cd, Co, Cr, Cu, Fe, Hg, Mn, Mo, Na, Ni, Pb, Se, Zn) (spring 2010)

(a)	DBO5 (mg L^{-1})						
	Autumn 2009	Winter 2010	Spring 2010	Autumn 2010	Winter 2011	Summer 2011	Autumn 2011
L1	n.a.	0	n.a.	3	n.m	8	9
L2	n.a.	1	n.a.	3	n.a.	19	n.a.
L3	n.a.	0	n.a.	3	n.m	n.m	n.a.
C	n.a.	n.a.	n.a.	n.a.	n.a.	3	n.a.
R	n.a.	n.a.	n.a.	n.a.	n.a.	n.a.	6

(b)	O_2 (mg L^{-1})						
	Autumn 2009	Winter 2010	Spring 2010	Autumn 2010	Winter 2011	Summer 2011	Autumn 2011
L1	4	13.20	9–80	13.20	n.m	10.08	n.a.
L2	5	13.08	8.63	13.60	n.a.	11.60	n.a.
L3	4	11.94	8.11	13.20	n.m	n.m	n.a.
C	n.a.	n.a.	5.37	n.a.	n.a.	n.a.	n.a.
R	n.a.	n.a.	n.a.	n.a.	n.a.	n.a.	n.a.

(c)	Solids in suspension (g L^{-1})						
	Autumn 2009	Winter 2010	Spring 2010	Autumn 2010	Winter 2011	Summer 2011	Autumn 2011
L1	0.02	0.03	0.02	n.a.	n.m	n.a.	n.a.
L2	0.16	0.04	0.04	n.a.	n.a.	n.a.	n.a.
L3	0.18	0.05	0.05	n.a.	n.m	n.a.	n.a.
C	n.a.	n.a.	0.01	n.a.	n.a.	n.a.	n.a.
R	n.a.	n.a.	n.a.	n.a.	n.a.	n.a.	n.a.

(d)	Redox potential (Eh) (mV)							
	Autumn 2009	Autumn (after rain)	Winter 2010	Spring 2010	Autumn 2010	Winter 2011	Spring 2011	Autumn 2011
L1	196	394	414	383	538	n.m	153	180
L2	319	304	411	357	470	335	272	n.a.
L3	231	388	390	345	456	n.m	n.m	n.a.
C	n.a.	n.a.	n.a.	335	n.a.	290	-6	n.a.
R	n.a.	n.a.	n.a.	n.a.	n.a.	n.a.	n.a.	n.a.

(e)	Alkalinity (meq L^{-1} H^+)							
	Autumn 2009	Autumn (after rain)	Winter 2010	Spring 2010	Autumn 2010	Winter 2011	Spring 2011	Autumn 2011
L1	1.30	0.57	0.30	0.99	0.21	n.m	1.44	2.58
L2	1.24	0.56	0.28	0.57	0.42	0.44	2.41	n.a.
L3	1.32	0.60	.30	0.88	0.25	n.m	n.m	n.a.
C	n.a.	n.a.	n.a.	0.99	n.a.	0.22	0.24	n.a.
R	n.a.	n.a.	n.a.	n.a.	n.a.	n.a.	n.a.	n.a.

(f)	DOC (mg L^{-1})							
	Autumn 2009	Autumn (after rain)	Winter 2010	Spring 2010	Autumn 2010	Winter 2011	Spring 2011	Autumn 2011
L1	20.60	2.27	2.83	4.16	n.a.	n.m	11.9	n.a.
L2	22.90	1.33	3.61	2.12	5.86	1.54	12.55	n.a.
L3	2.77	1.06	3.75	5.10	n.a.	n.m	n.m	n.a.

Table 1 (continued)

(f)	DOC (mg L^{-1})							
	Autumn 2009	Autumn (after rain)	Winter 2010	Spring 2010	Autumn 2010	Winter 2011	Spring 2011	Autumn 2011
C	n.a.	n.a.	n.a.	7.32	n.a.	< 0.50	6.17	n.a.
R	n.a.	n.a.	n.a.	n.a.	n.a.	n.a.	n.a.	n.a.
(g)	NH_4^+ (mg L^{-1})							
	Autumn 2009	Autumn (after rain)	Winter 2010	Spring 2010	Autumn 2010	Winter 2011	Spring 2011	Autumn 2011
L1	< 0.05	< 0.05	< 0.05	< 0.05	< 0.05	n.m	< 0.05	n.a.
L2	< 0.05	< 0.05	< 0.05	< 0.05	< 0.05	0.32	< 0.05	n.a.
L3	0.37	< 0.05	< 0.05	< 0.05	< 0.05	n.m	n.m	n.a.
C	n.a.	n.a.	n.a.	< 0.05	n.a.	0.32	0.09	n.a.
R	n.a.	n.a.	n.a.	n.a.	n.a.	n.a.	n.a.	n.a.
(h)	NO_2^- (mg L^{-1})							
	Autumn 2009	Autumn (after rain)	Winter 2010	Spring 2010	Autumn 2010	Winter 2011	Spring 2011	Autumn 2011
L1	< 0.02	< 0.02	< 0.02	0.02	0.07	n.m	0.02	n.m
L2	< 0.02	< 0.02	< 0.02	< 0.02	0.03	< 0.02	0.03	n.m
L3	< 0.02	< 0.02	< 0.02	0.05	0.08	n.m	n.m	n.m
C	n.a.	n.a.	n.a.	< 0.02	n.a.	< 0.02	< 0.02	n.a.
R	n.a.	n.a.	n.a.	n.a.	n.a.	n.a.	n.a.	n.a.
(i)	NO_3^- (mg L^{-1})							
	Autumn 2009	Autumn (after rain)	Winter 2010	Spring 2010	Autumn 2010	Winter 2011	Spring 2011	Autumn 2011
L1	0.11	0.05	6.26	< 1.00	n.a.	n.m	0.75	n.a.
L2	0.11	0.06	4.47	< 1.00	< 1.00	n.a.	0.65	n.a.
L3	0.10	0.06	3.21	< 1.00	n.a.	n.m	n.m	n.a.
C	n.a.	n.a.	n.a.	< 1.00	n.a.	202	6.02	n.a.
R	n.a.	n.a.	n.a.	n.a.	n.a.	n.a.	n.a.	n.a.
(j)	PO_4^{3-} (mg L^{-1})							
	Autumn 2009	Autumn (after rain)	Winter 2010	Spring 2010	Autumn 2010	Winter 2011	Spring 2011	Autumn 2011
L1	< 0.05	0.05	< 0.05	< 0.05	< 0.05	n.m	< 0.05	n.a.
L2	0.05	0.05	< 0.05	0.14	0.14	0.14	< 0.05	n.a.
L3	0.05	< 0.05	< 0.05	0.85	0.05	n.m	n.m	n.a.
C	n.a.	n.a.	n.a.	< 0.05	n.a.	0.18	< 0.05	n.a.
R	n.a.	n.a.	n.a.	n.a.	n.a.	n.a.	n.a.	n.a.
(k)	Cl^- (mg L^{-1})							
	Autumn 2009	Autumn (after rain)	Winter 2010	Spring 2010	Autumn 2010	Winter 2011	Spring 2011	Autumn 2011
L1	137	828	47.2	67.5	95.8	n.m	200	n.a.
L2	145	82.3	47.0	58.1	94.8	134.0	257	n.a.
L3	119	86.7	47–5	63.0	101	n.m	n.m	n.a.
C	n.a.	n.a.	n.a.	251.97	n.a.	2636	68.8	n.a.
R	n.a.	n.a.	n.a.	n.a.	n.a.	n.a.	n.a.	n.a.

Table 1 (continued)

(l)	SO_4^{2-} (mg L^{-1})							
	Autumn 2009	Autumn (after rain)	Winter 2010	Spring 2010	Autumn 2010	Winter 2011	Spring 2011	Autumn 2011
L1	2.43	3.76	10.53	7.00	22.76	n.m	23.10	n.a.
L2	2.25	3.38	9.98	< 2.50	21.31	12.05	18.30	n.a.
L3	2.29	3.40	9.05	< 2.50	26.22	n.m	n.m	n.a.
C	n.a.	n.a.	n.a.	19.37	n.a.	538	6.78	n.a.
R	n.a.	n.a.	n.a.	n.a.	n.a.	n.a.	n.a.	n.a.

(m)	Trace metals (Spring 2010) (μg L^{-1})													
	As	Cd	Co	Cr	Cu	Fe	Hg	Mn	Mo	Na	Ni	Pb	Se	Zn
L1	0.98	0.016	0.05	0.18	0.53	5.56	0.15	6.75	0.19	30,828.55	0.29	0.05	0.33	2.99
L2	0.61	0.022	0.06	0.19	1.10	15.66	0.14	25.78	0.23	29,466.36	0.21	0.01	0.23	1.13
L3	1.09	0.011	0.10	0.18	1.54	10.71	0.11	48.96	0.19	33,354.48	0.66	0.12	0.21	1.09
C	0.80	0.028	0.08	0.27	2.03	19.79	0.14	36.83	0.14	86,052.51	0.32	0.07	0.51	1.38
R														

The TC and TS content in sediments were determined by granulometry: in both cases, values were higher in the upper levels, with a higher proportion of fine fractions. No seasonal differences were observed in TC and TS contents in sediment profiles. TC ((1.0) 6.0–36.5%) and TS content (0.31–1%) were higher in the upper levels but drastically stabilized around the minimum values (TC < 0.5%, TS < (0.1) 0.2%) in deep layers, consistently with the higher proportion of sands, although this stabilization occurred more progressively in the vegetated zone dominated by *S. lacustris* (Fig. 4). TS content showed an increase in the lower levels in all the profiles and in the intermediate levels in the case of the central zone, consistently with the presence of black mottles that corresponded to iron sulfides, pyrite (FeS_2) or pyrite metastable forms (FeS and Fe_2S_3) (Fig. 4). The S:C ratio was low in all profiles and values were within the range of freshwater sediments (Fig. 5).

The pH value of the reaction (pH) showed mean circumneutral values ranging from slightly acidic (4.6) to alkaline (8.3), as summarized in Fig. 6. pH values were slightly acidic, showing a drastic increase to slightly alkaline values at a depth of 60–80 cm in the central zone and at a depth of 20–25 cm in the *S. lacustris* zone. However, pH remained stable at slightly acidic values (5.3–7.0) in the *P. australis* zone. Redox potential (Eh) ranged between 0 and 450 mV, with minimum values in winter and increasing values towards autumn; black mottles were also detected in deep levels, with lower redox potential values in all profiles (Fig. 6). Electrical conductivity (E.C.) showed higher values surface levels of the profiles, stabilizing around minimum values in the deeper levels in all the profiles. Electrical conductivity (E.C.) fluctuated between 0.04 and 3.45 dS m^{-1}, with higher values in the upper levels of the central zone than in vegetation zones dominated by helophytes *S. lacustris* and *P. australis.* Moreover, the highest values were found in the upper levels for all profiles, stabilizing around minimum values in the deeper levels regardless of seasonality (Fig. 6). Seasonal fluctuations in E.C. in the upper levels were wider in the central zone than in the vegetated zone dominated by helophytes; in the upper levels, values decreased seasonally from spring to autumn in the central zone but showed no oscillations in the vegetated zones dominated by both helophytes. pH, electrical conductivity (E.C.) and redox potential (Eh) values showed a marked change in lower levels in all profiles, specifically at a depth > 50 cm in the central zone and > 20 cm in the vegetated zones dominated by both helophytes.

The proportion of clay fraction and organic matter was inverse with depth of the sedimentary profile. Fractions F3 and F5 of P, F2 and F3 of Fe, and F2 of Cu show higher values with the increasing percentage of clay fraction in the sediment. F1 and F3 of Fe, F1–F3 of Mn and all fractions of Cu and P, except for F4 of P, showed a with the increasing of organic matter (TC, TS) in sedimentary profiles. F1 of Fe showed a positive correlation with all fractions of P, with the exception of F4. In addition, F4 of P (apatite), Fe and Mn (pyrite) showed higher values with the increasing proportion of sand fraction in the sediment.

Phosphorus dynamics in sediments

Phosphorus concentration in the central zone was as follows: F5 = F3B > F3 > (F4 > F2 > F1). The results

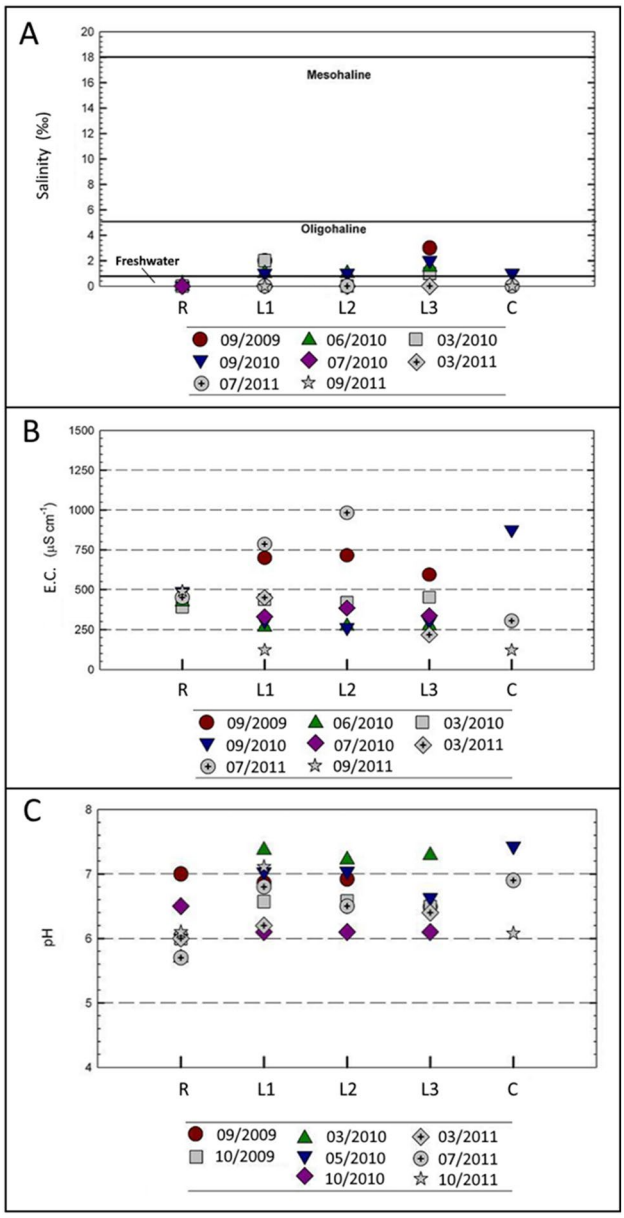


Fig. 2 Spatial and temporal variation of the main chemical parameters in the water of Xuño Lake (2009–2011): **a** salinity (‰), **b** electrical conductivity (E.C) (µS cm^{-1}) and **c** pH at the sampling points in Xuño Lake

showed that phosphorus was mainly associated with F5, refractory organic matter, and F3B, humic acids. F5 showed a peak concentration of 2.2–24 µmol g^{-1} (summer)/12–27.8 µmol g^{-1} (autumn) in the upper levels, with a higher proportion of fine fractions at a depth < 20 cm, with a steep decline < 3 µmol g^{-1} in the lower levels, at a depth of > 20 cm. F3B showed a peak of P overlapping with F5 in upper levels, with high values [5–21.8 µmol g^{-1} (summer)/12.3–25.8 µmol g^{-1} (autumn)] at a depth < 20 cm, with a steep decline < 1 µmol g^{-1} in the lower levels, at a depth of > 20 cm. F3 had maximum values of 2 µmol g^{-1} on the surface with but dropped abruptly to < 0.05 µmol g^{-1} in depth. F4 showed low concentrations (< 2 µmol g^{-1}) along all profiles, but unlike the other fractions, the highest values were found in the lower levels of profiles: 0.9 µmol g^{-1} at a depth of 72 cm and 1.2 µmol g^{-1} at a depth of 101 cm. F2 and F1 showed very low concentrations: < 0.5 µmol g^{-1} (summer)/ < 2.25 µmol g^{-1} (autumn) and < 0.05 µmol g^{-1}, respectively, although values decreased to < 0.1 µmol g^{-1} at a depth > 10 cm (Fig. 7).

The ^{31}P NMR spectra showed that the dominant form of P extracted with NaOH–EDTA in the central zone was monoester phosphorus (381–544 mg kg^{-1}) > orthophosphate (399–414 mg kg^{-1}) > diester phosphorus (10–147 mg kg^{-1}) > pyrophosphate (7–44 mg kg^{-1}), both on the surface and in depth in sedimentary profiles. Phosphorus extracted with NaOH–EDTA in sediments from the *P. australis* zone showed the same pattern as those from the central zone; however, in the *S. lacustris* zone, orthophosphate was predominant (52–541 mg kg^{-1}), followed by monoester phosphorus (287 mg kg^{-1}), diester phosphorus (< 25 mg kg^{-1}), and pyrophosphate (< 10 mg kg^{-1}) (Fig. 7).

Iron dynamics in sediments

Iron (Fe) concentration in the central zone and in the zones dominated by both helophytes was as follows: F3 > F2 > F1 > F4, with higher contents of all iron fractions in the upper levels of all profiles. Seasonally, iron concentration of fractions F1, F2 and F4 decreased from spring to autumn, although F3 showed a high increase in all profiles (Fig. 8).

Table 2 Summary of microbiological data from the water of Xuño Lake (2010–2011): total coliforms, faecal coliforms, faecal Streptococci, and total aerobic bacteria (25 ºC/37 ºC)

Date	Total Coliforms (UFC 100 ml^{-1})	Faecal Coliforms (UFC 100 ml^{-1})	Faecal Streptococci (UFC 100 ml^{-1})	Total aerobic (25 ºC) (UFC ml^{-1})	Total aerobic (37 ºC) (UFC ml^{-1})
05/2010	13	66	30	6.6×10^2	5.5×10^2
10/2010	$> 10^4$	190	290	2.5×10^3	2.7×10^3
10/2011	21	540	69	$> 10^4$	6.8×10^3

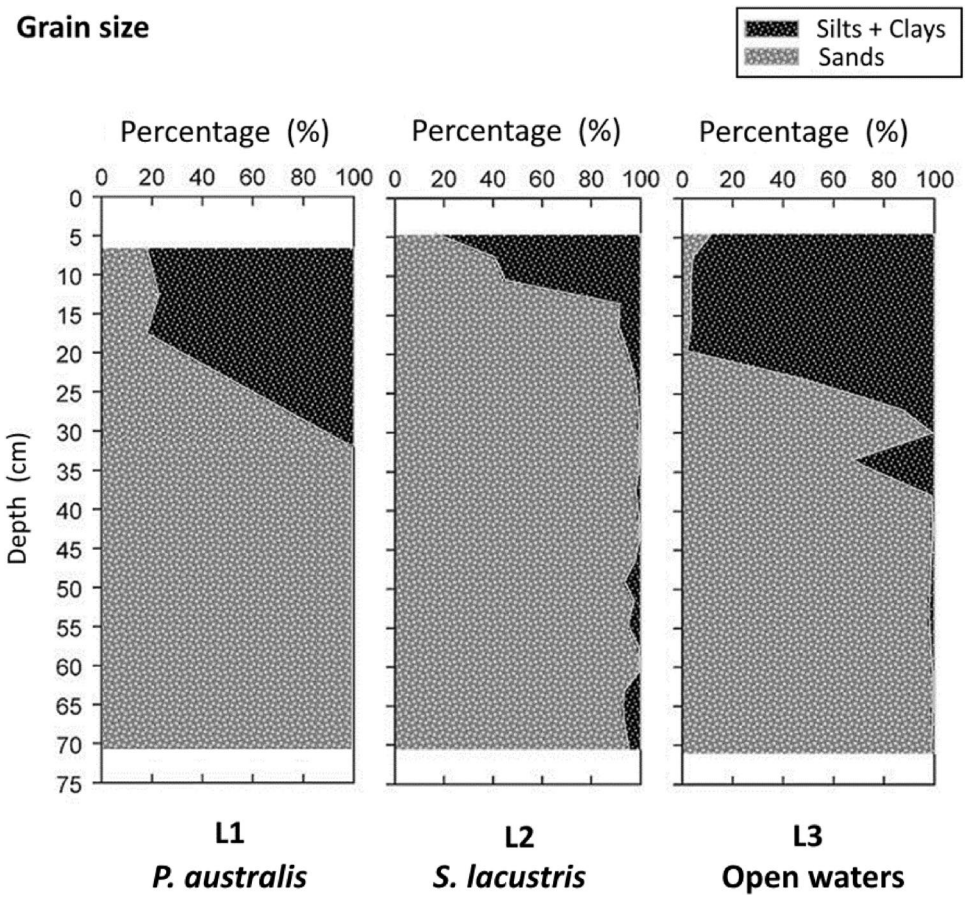


Fig. 3 Grain size analysis of sediment profiles from Xuño Lake against depth in the three sampling points within the lake: L1—*P. australis* area, L2—*S. lacustris* area and L3—open waters

The values in the *P. australis* zone were as follows: F1: 2–30 µmol g^{-1} (< 17 cm) and 0.01–0.11 µmol g^{-1} (> 17 cm); F2: 3–37 µmol g^{-1} (< 17 cm) and < 2 µmol g^{-1} (> 17 cm); F3: 240–628 µmol g^{-1} (< 17 cm) and < 3 µmol g^{-1} (> 17 cm); and F4: 0.25–0.64 µmol g^{-1} (< 8 cm) and 0.01–0.15 µmol g^{-1} (> 8 cm). F3 showed a high increase, with a subsurface peak up to 628 µmol g^{-1} (< 17 cm) towards the autumn. In addition, F1 and F2 had a maximum peak of 0.84 µmol g^{-1} at a depth of 10–20 cm, while F4 had an increase up to 0.15 µmol g^{-1} at lower levels towards the autumn (Fig. 8).

As for the *S. lacustris* zone, the values were the following: F1: 0.14 µmol g^{-1} (< 10 cm), with subsurface maximum values and 0.01–0.02 µmol g^{-1} (> 10 cm); F2: 6–25 µmol g^{-1} (< 10 cm) and < 4 µmol g^{-1} (> 10 cm); F3: 284–296 µmol g^{-1} (< 10 cm) and 9–79 µmol g^{-1} (> 10 cm); and F4: 0.1–0.36 µmol g^{-1} (< 3 cm) and 0.01–0.04 µmol g^{-1} (> 3 cm). F3 showed a high increase towards the surface, with a peak of up to 500 µmol g^{-1} (0–22.5 cm) in autumn (Fig. 8).

The central zone showed the following values: F1: 0.38–69 µmol g^{-1} (< 25 cm), with a subsurface maximum and 0.17–3.10 µmol g^{-1} (> 25 cm); F2: 20–88 µmol g^{-1} (< 25 cm) and < 5 µmol g^{-1} (> 25 cm), with slight, irregular increases between 40 and 50 cm; F3: 167–324 µmol g^{-1} (< 25 cm) and 2–45 µmol g^{-1} (> 25 cm), with slight, irregular increases of up to 31 µmol g^{-1} (40–50 cm) or 0.38 µmol g^{-1} (59–62.5 cm); F4: 0.38 µmol g^{-1} (< 5 cm) and < 0.1 µmol g^{-1} (> 5 cm), although with a seasonal peak of 164 µmol g^{-1} in spring in the lower levels (45–50 cm). F2 and F3 showed peaks towards the sediment surface, up to 424 µmol g^{-1} for F3 (0–1 cm). Conversely, F1 and F4 showed peaks in depth: F1 with 0.31 µmol g^{-1} at 38 cm and F4 with 49 µmol g^{-1} at 38 cm and with an abrupt decrease of 0.17 µmol g^{-1} at 50.5 cm (Fig. 8).

Manganese dynamics in sediments

Manganese (Mn) concentrations in the central zone and in the zones dominated by both helophytes were as follows: F1 = F3 > F2 > F4, with higher contents of all manganese fractions in the upper levels with greater proportions of fine for all profiles: central zone at a depth < 22.5(27.5) cm, *P. australis* zone at a depth < 17 cm and *S. lacustris* zone at a depth < 10 cm. Seasonally, F1 was dominant in the area covered by *P. australis,* while F3 was dominant in the central zone and in the area covered by *S. lacustris* in the sedimentary profiles (Fig. 9).

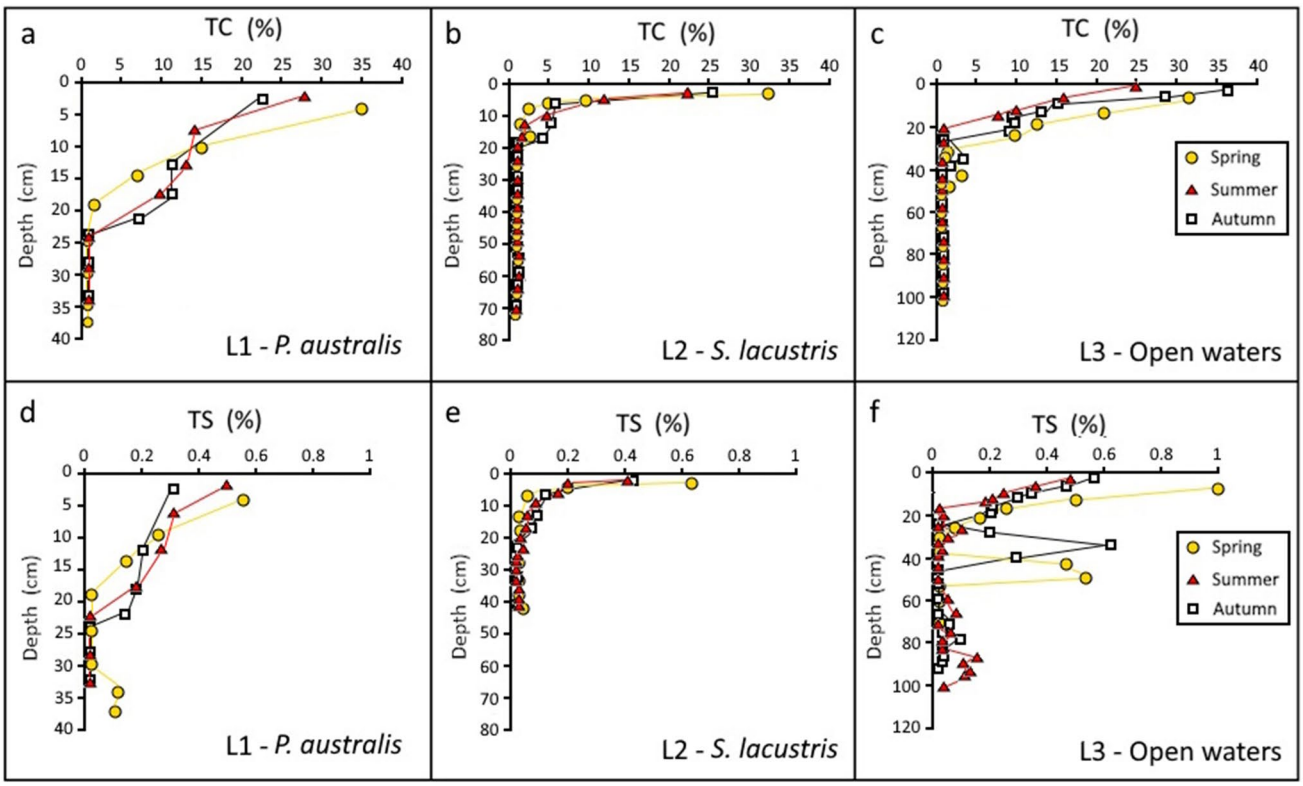


Fig. 4 Spatial and temporal variation of **a–c** total carbon (TC) and **d–f** total sulphur (TS) contents in sediment profiles from Xuño Lake against depth in the three sampling points within the lake and in three different seasons (spring, summer and autumn 2011): L1—*P. australis* area, L2—*S. lacustris* area and L3—open waters

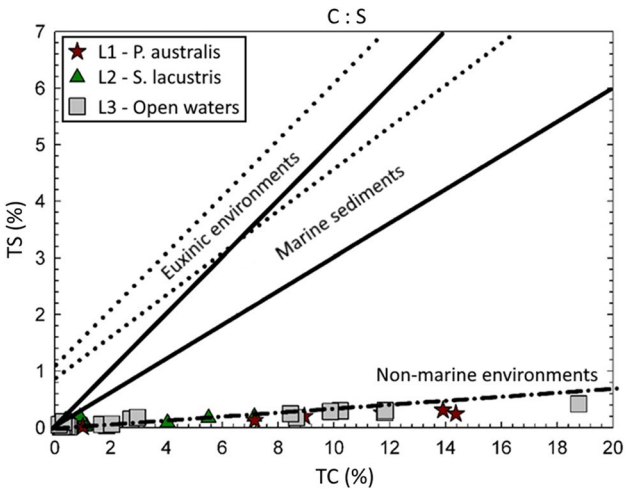


Fig. 5 Relationship between total S and total organic C in sediments from Xuño Lake in the three spatial sampling points (i.e., L1—*P. australis* area, L2—*S. lacustris* area and L3—open water). The solid black lines represent the typical relationship for modern marine sediments (C:S = 2.8 ± 1.5, Berner 1982; Berner and Raiswell 1984), while the dotted line represents the same relationship for euxinic environments and the dot–dashed line represents the typical relationship in freshwater environments with low sulphate concentrations (Leventhal, 1995)

In the *P. australis* zone, in the upper levels of the profiles (< 17 cm), concentrations of manganese were: F1: 180–1270 nmol g^{-1} (spring)/30–110 nmol g^{-1} (summer–autumn), with 10–14 nmol g^{-1} in the lower levels; F2: 30–80 nmol g^{-1} (spring)/85–144 nmol g^{-1} (summer–autumn); F3: 330–400 nmol g^{-1} (spring)/430–720 nmol g^{-1} (summer–autumn), with 10–59 nmol g^{-1} in the lower levels; F4: < 0.1 nmol g^{-1} throughout the whole profile (Fig. 9).

The values in the *S. lacustris* zone were as follows: F1: 310–2723 nmol g^{-1}, with < 53 (100) nmol g^{-1} in the lower levels (spring)/16(86)–1184 nmol g^{-1} (summer–autumn); F2: 173–474 nmol g^{-1}, with < 10 nmol g^{-1} in the lower levels (spring)/21–219 nmol g^{-1} (summer–autumn); F3: 424–578 nmol g^{-1}, with < 121 nmol g^{-1} in the lower levels (spring)/168–2946 nmol g^{-1} (summer–autumn), with < 6 nmol g^{-1} (summer)/27–39 nmol g^{-1} (autumn) in the lower levels; F4: < 15 nmol g^{-1} (summer) or < 5 nmol g^{-1} (autumn) in the upper levels and < 0.1 nmol g^{-1} throughout the profile in the lower levels (Fig. 9).

In the central zone, ain the upper levels of the profiles (< 22.5(27.5) cm), the manganese concentrations showed the following values: F1: 357–4552 nmol g^{-1} (spring)/79–1381 nmol g^{-1} (summer–autumn) (< 22.5 cm)

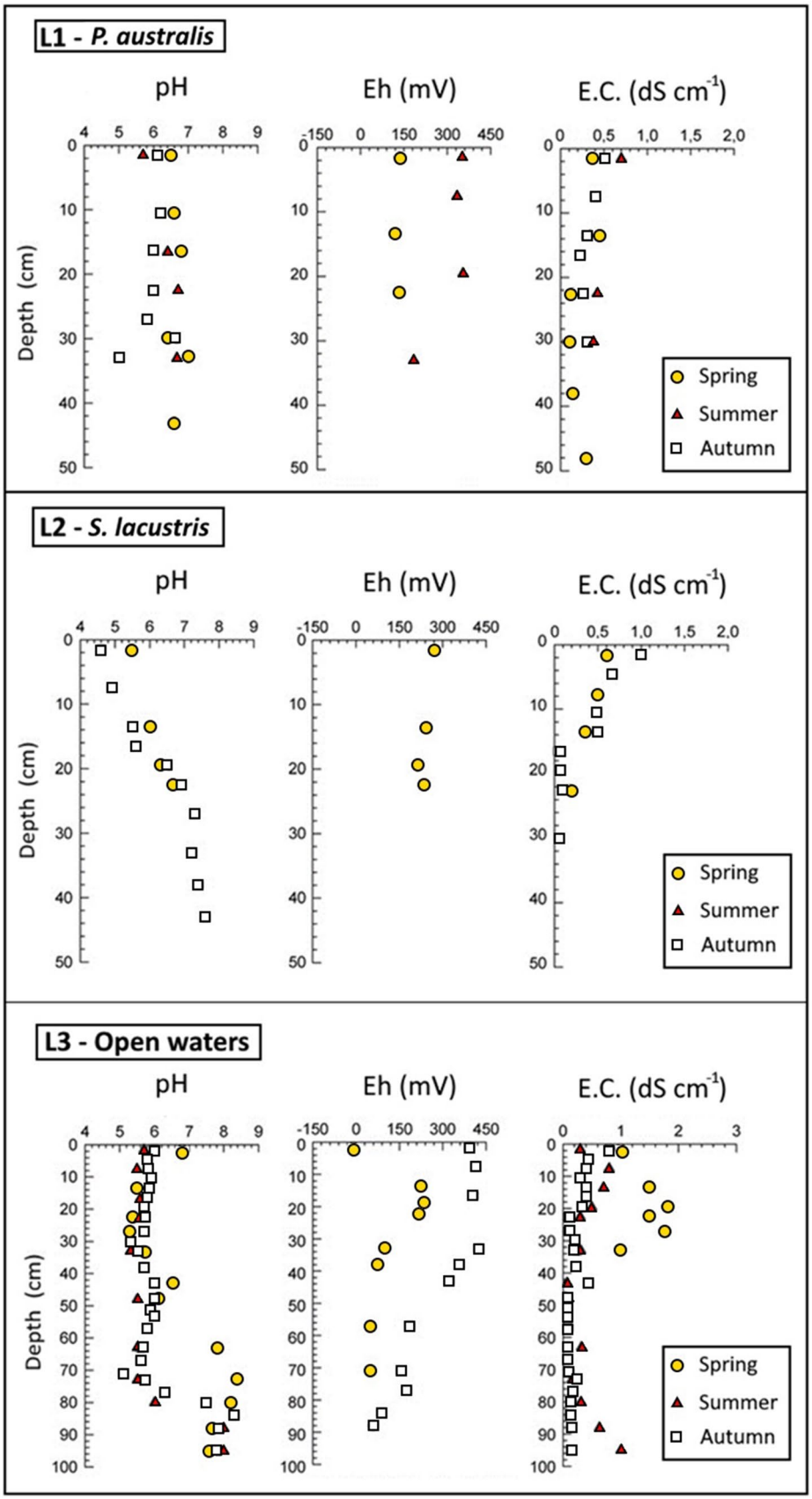


Fig. 6 Spatial and temporal variations in pH, redox potential (mV) and electrical conductivity (EC) (μS cm^{-1}) in sediment profiles from Xuño Lake against depth in the three sampling points within the lake and in three different seasons (spring, summer and autumn 2011): L1—*P. australis* area, L2—*S. lacustris* area and L3—open waters

with 25 nmol g^{-1} in lower levels; F2: 108–352 nmol g^{-1} (spring)/163–3459 nmol g^{-1} (summer–autumn) (< 22.5 cm); F3: 185–569 nmol g^{-1} (< 27.5 cm)/200–3758 nmol g^{-1} (summer–autumn); F4: < 0.1 nmol g^{-1} throughout the profile. The lower levels with a higher proportion of sand had manganese values < 1 (5) nmol g^{-1}, with the exception of F4, with a peak up to 48 nmol g^{-1} at a depth of 88.5 cm in summer and 100 nmol g^{-1} at a depth of 47 cm in autumn (Fig. 9).

Copper and Cobalt dynamics in sediments

Copper (Cu) concentrations in the central zone were as follows: F4 (high in spring)/F3 (high in summer) > F1 > F2, with a higher content of all Cu fractions in the upper levels with higher proportions of fine fractions in all profiles. Cu showed a high degree of pyritization in spring but it decreased in summer; therefore, Cu showed a different dynamic than Fe and Mn (Fig. 10).

Copper (Cu) concentrations in the upper levels of the profiles were the following: F1: < 0.1 nmol g^{-1} up to < 37.5 cm), with irregular increases 42.5–62 cm and a peak of 78 nmol g^{-1} at a depth of 47.5 cm; F2: < 8.7 nmol g^{-1} (spring)/ < 3 nmol g^{-1} (summer) throughout the profile; F3: 13–27 nmol g^{-1} (< 22.5 cm) (spring)/48–202 nmol g^{-1} (summer), with a steep decline < 5 nmol g^{-1} throughout the profile; F4: 390 nmol g^{-1} (< 10 cm) (spring)/ < 70 nmol g^{-1} (< 22.5 cm) (summer), with a steep decline up to 7–13 nmol g^{-1} at a depth of 12.5–22.5 cm and a slight increase up to 33 nmol g^{-1} at a depth of 42.5–47.5 cm (Fig. 10).

Cobalt (Co) showed the highest concentrations in F3: 1.5–19 nmol g^{-1} (< 50 cm) (spring)/8.7–20.4 nmol g^{-1} (< 20 cm) (summer) in the upper levels with the highest proportion of fine fractions and < 0.1 nmol g^{-1} in the lower levels (Fig. 10). Co concentrations in F1, F2 and F4 were below the detection limit (< 0.1 nmol g^{-1}).

Discussion

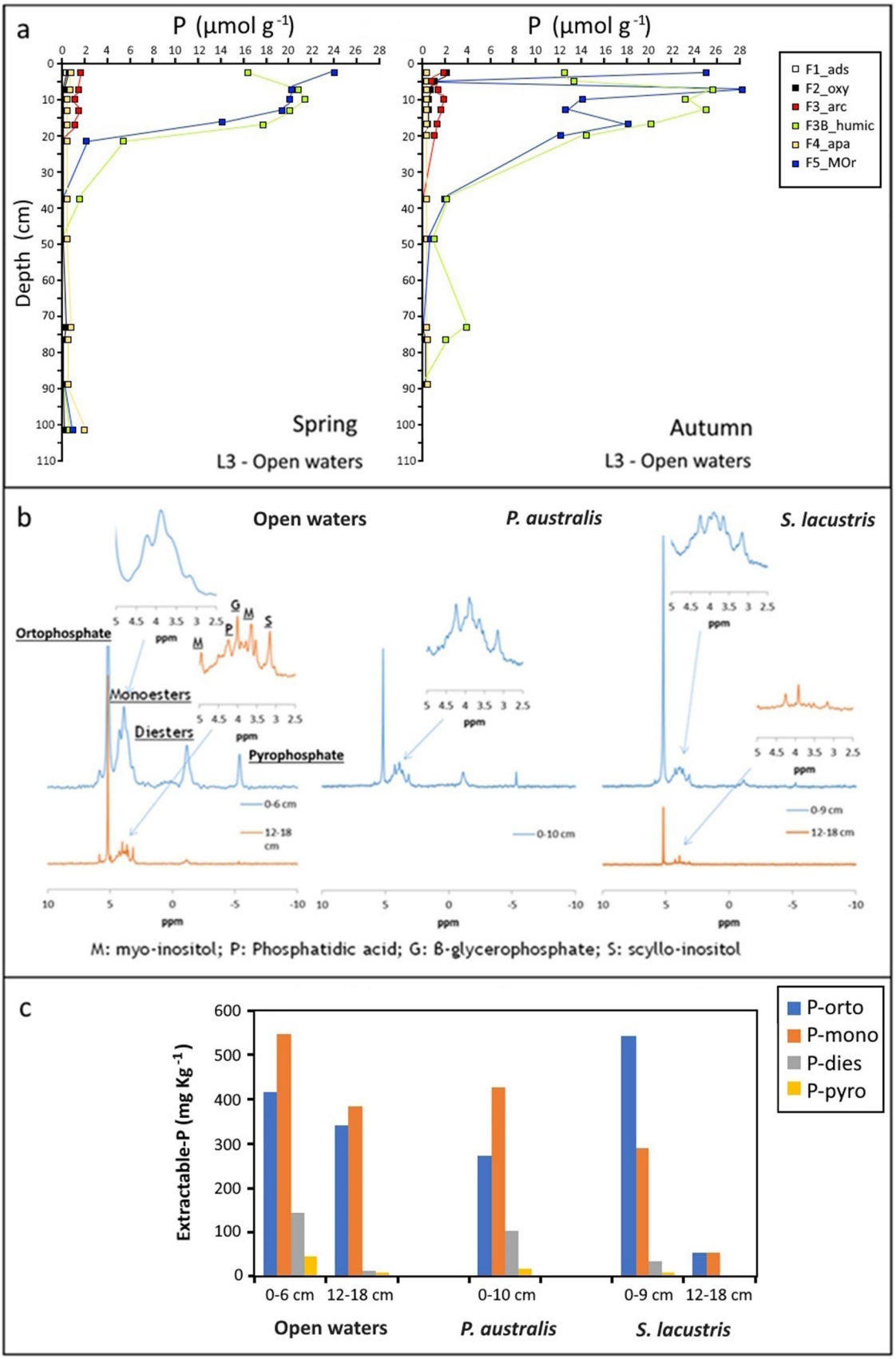
Trophic status of Xuño Lake

The composition and parameters of the water in Xuño Lake showed values typical of poorly mineralised (0.5 dS cm^{-1}) freshwaters in Iberian siliceous rock areas with no marine influence (Membiela et al. 1991), although with an increase in salinity (2 dS cm^{-1}) and suboxia/anoxia (< 10%) associated with a water deficit and higher evaporation rates during the summer. The small volume and the important seasonal fluctuations in the hydrological regime of Xuño Lake make the ecological status of the wetland very sensitive to any human disturbance. The concentration of metals and metalloids (i.e., As, Cd, Co, Cr, Cu, Fe, Hg, Mn, Mo, Na, Ni, Pb, Se, Zn) (Table 1) and sediments (i.e., Fe, Mn, Cu, Co) (Figs. 8, 9 and 10) showed values below the contamination threshold: As = 25 µg l^{-1}, Cd = 1–3 µg l^{-1}, Co = 1 µg l^{-1} (1.69 10^9 nmol g^{-1} in sediments), Cr = 3.4–4.7 µg l^{-1}, Cu = 5–30 µg l^{-1} (1.57 10^9 nmol g^{-1} in sediments), Fe = no limit (179 10^6 µmol g^{-1} in sediments), Hg = 0.07 µg l^{-1}, Mn = µg l^{-1} (91 10^6 µmol g^{-1} in sediments), Mo = 70 µg l^{-1}, Na = no limit, Ni = 4 µg l^{-1}, Pb = 1.2 µg l^{-1}, Se = 1 µg l^{-1}, Zn = 5–100 µg l^{-1} (ATSDR 2004; Bernárdez et al. 2017; Smedley and Kinniburgh 2017; Nag and Cummins 2021).

However, Hg shows slightly high levels in the lake and channel water (0.11–0.15 µg l^{-1}), twice the established threshold value for Hg in water for human use (0.07 µg l^{-1}) (Nag and Cummins 2021), although there are no human activities in the Xuño Lake basin that can cause mercury contamination. In fact, Hg levels in natural freshwater wetlands in the Iberian Peninsula are below 0.05 µg l^{-1}, such as the Ebro river (Fernández-Gómez et al. 2012; Sierra et al. 2017) or unpolluted mountain lakes of the Pyrenees (Duval et al. 2023), although mercury concentrations ranging from 0.01 to 0.10 µg/L have also been reported for unpolluted lakes and rivers in Canada (D'Itri 1972).

Mercury (Hg) have a strong affinity with organic compounds and clays suspended; therefore, this causes the accumulation of Hg in the sediments and very low levels in water (D'Itri 1972; Nag and Cummins 2021). However, anoxia in the water column changes the reduction–oxidation conditions favoring the release of Hg from the sediment (Branfireun et al. 2020), and the Hg levels recorded in the water of Xuño Lake in the spring of 2010 can be explained by the suboxic conditions in the water column (< 10% oxygen saturation) during the summer period, since the lake is shallow and has a small volume (Table 1). The anoxic conditions of the water limit microbial activity and favor the increase of dissolved organic matter (Sobek et al. 2009; Lau and Del Girogio 2020), as shown by the high DOC values in spring–autumn in the Xuño Lake (Table 1) and, therefore, also contribute to the increase of Hg in water due to its strong affinity for organic compounds. In anoxic sediments and water, the bioavailability of Hg are largely governed by reactions between Hg(II), inorganic sulfides, and natural organic matter (Gu et al. 2011; Hsu-Kim et al. 2013). However, the Hg levels registered in the water of Lake Xuño are the result of natural fluctuations, so they cannot be considered contamination.

The observed BOD5 and microbial load suggest a high input of nutrients of organic origin. However, the chemical and microbiological parameters below the contamination thresholds in the tributary river, as well as the low population density in the lake basin and the absence of wastewater discharges, does not allow identifying the origin of the contamination source. The faecal coliform: streptococci ratio


a
P (µmol g-1)
P (µmol g-1)
Depth (cm)
F1_ads
F2_oxy
F3_arc
F3B_humic
F4_apa
F5_MOr
Spring
L3 - Open waters
Autumn
L3 - Open waters
b
Open waters
P. australis
S. lacustris
Ortophosphate
Monoesters
Diesters
Pyrophosphate
0-6 cm
12-18 cm
0-10 cm
0-9 cm
12-18 cm
ppm
M: myo-inositol; P: Phosphatidic acid; G: ß-glycerophosphate; S: scyllo-inositol
c
Extractable-P (mg Kg-1)
P-orto
P-mono
P-dies
P-pyro
0-6 cm
12-18 cm
0-10 cm
0-9 cm
12-18 cm
Open waters
P. australis
S. lacustris

◂**Fig. 7** Spatial and temporal variations in P content (μmol g^{-1}) in sediment profiles from Xuño Lake against depth in 2011: **a** P content in open water sediment profiles of Xuño Lake against depth in two different seasons (spring and summer): F1—soluble and adsorbed P; F2—P adsorbed on Fe oxides and hydroxides; F3—P associated with silica clay minerals and Al hydroxides; F3B—P associated with humic acids; F4—P linked to apatite; F5—P associated with refractory organic matter; **b** content of P forms in three sampling points within the lake (L1—*P. australis* area, L2—*S. lacustris* area and L3—open waters); and **c** ^{31}P NMR spectrum obtained for the organic P fraction of the sediments in the soluble fraction extractable with NaOH–EDTA

ranging from 0.6 to 7.8 indicates a contamination of mixed origin. High values > 4.4 indicate faecal contamination of human origin, while values < 1 are typical of contamination of animal origin (Fraga-Santiago et al. 2019). Values around 0.6 are associated with avian faecal inputs related to the presence of ducks and gulls inhabiting the lake, as the high N and P contents in bird faeces can lead to a high disturbance of a small wetland ecosystem (Otero and Fernández-Sanjurjo 1999; Ligeza and Smal 2003; Peña-Lastra et al. 2022). Phosphorus is especially important to determine the trophic status in freshwater environments as the main limiting element (Poikane et al. 2019), because it is immobilized in sediments, together with Fe, under oxic conditions, leading to its reduced bioavailability in water (Blomqvist et al. 2004). However, the N and P levels of 0.14 mg l^{-1} in the water of Xuño Lake is below the eutrophication thresholds (Table 1): 0.3 mg l^{-1} for TP/phosphates, 5 mg l^{-1} for nitrates and 0.5 mg l^{-1} for nitrites and ammonium (Poikane et al. 2019), although studies on multiple lake ecosystems in Germany and the British Isles has established an optimal range of 0.011–0.075 mg l^{-1} TP (Willby et al. 2012; Dolman et al. 2016; Free et al. 2016).

Sediment biogeochemistry, through bottom-up regulation, plays a key role in the trophic status of wetlands as sinks for organic matter, nutrient and metals (Benndorf et al. 2002). The composition of the Xuño Lake sediments is determined by their granulometry, with a higher proportion of fine sediments in the upper levels (Fig. 3). This entails a high content of organic matter (Figs. 4a–c, 5), sulphur (TS) (Figs. 4d–f, 5), nutrients (P) (Fig. 7) and the main trace metals: Fe, Mn, Cu and Co (Table 1; Figs. 8, 9 and 10). In addition, the high TC:TS ratio (Fig. 5) indicates that the lake sediments were originated from inland water environments (Benndorf et al. 2002; Hickey and Gibbs 2009; Sinistro 2010; Carey and Rydin 2021).

Low pH and anoxic conditions favour the release of P in sediments and its diffusion in the water column (Blomqvist et al. 2004). The lowest pH values (4–7) were associated with samples with the highest organic matter contents, absence of carbonates and presence of metastable Fe sulfides. The redox potentials observed in fine texture sediment samples correspond with suboxic environments and fluctuated seasonally between oxic conditions in spring (Eh = 424 mV) and strongly reduced conditions (Eh = – 9 mV) in autumn. The bottom levels of sediment profiles with lower oxygen concentrations and low redox potential values are indicative of anoxic conditions, as evidenced by the black specks of metastable Fe sulfides and by an intense odor of hydrogen sulfide (SH_2) (Huerta-Díaz et al. 1998).

Phosphorus in sediments is mainly associated with organic matter (F5) and humic acids (F3B), since the high annual biomass productivity of macrophytes and suboxic conditions lead to enrichment of organic matter in sediments (Jeppesen et al. 1997), and organic P, such as orthophosphate diesters, can be degraded under anoxic conditions to inorganic P that are subsequently uptaken by macrophytes (Labry et al. 2002; Turner and Newman 2005; Joshi et al. 2015; Tu et al. 2019). Secondarily, P associated with clay and Al hydroxides (F3) is the following dominant fraction and is highly bioavailable for macrophytes (Paludan and Morris 1999; Jiménez-Cárceles and Álvarez-Rogel 2008; Jiménez-Cárceles et al. 2011; Nóbrega et al. 2014; Yu et al. 2022). In fact, both helophyte species, *P. australis* and *S. lacustris,* are very efficient in terms of nutrient absorption, especially N and P, and are widely used species in the design of artificial wetlands for wastewater treatment (Toet et al. 2005). No differences were observed in P content and dynamics in sediments between the open water area and helophyte-dominated areas, both with *P. australis* and with *S. lacustris*. However, there were differences in the predominance of organic forms of P in sediments, with higher P monoester concentrations in open waters and in the *P. australis* area, while P orthophosphate levels were higher in the *S. lacustris* area (Fig. 7), which may suggest different physiological preferences in terms of P uptake from sediments between both helophyte species (Carrillo et al. 2021).

Metals in sediments

The highest concentrations were in the upper levels of all profiles, associated with the highest proportion of fine fractions (Figs. 8, 9 and 10). Vegetation cover or the helophyte species present did not alter the spatial distribution of Fe and Mn levels in sediment profiles (Figs. 8, 9). F3, associated with Fe oxides and hydroxides, was the predominant one for Fe and Co in sediments from Xuño Lake.

The drop in water level in the central zone towards the summer generates oxic conditions (Eh > 350 mV) in the water and in surface sediment due to the high photosynthetic activity. The greater aeration of the system causes the oxidation of reduced Fe forms, which in turn leads to an increase in Fe(III) oxyhydroxides in the surface portion of the substrate, to the clear detriment of the contents of exchangeable Fe and Fe sulfides, in comparison with the results obtained in the maximum water level period during the spring.

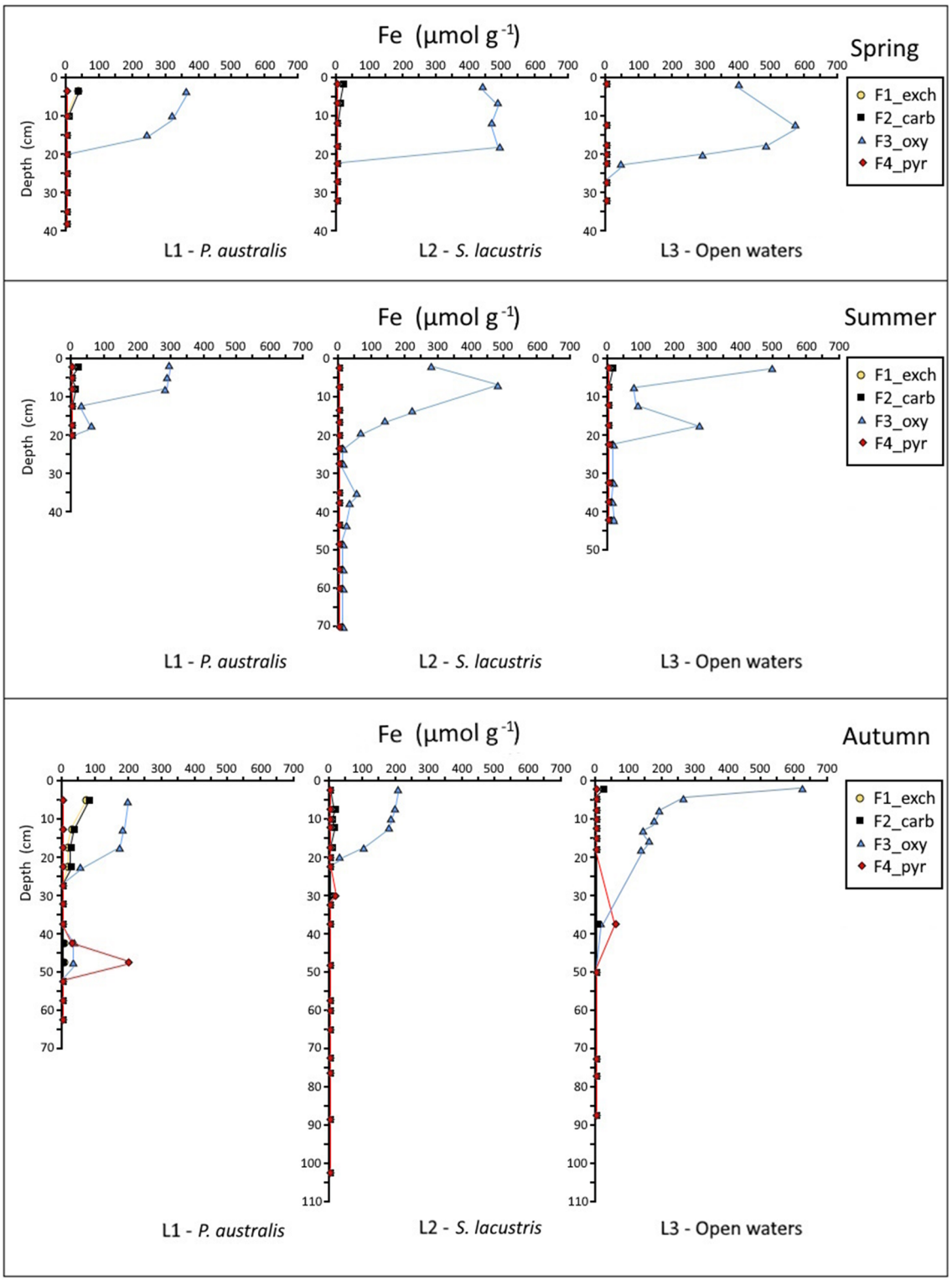


Fig. 8 Spatial and temporal variations in the contents of different Fe fractions (µmol g^{-1}) in open-water sediment profiles from Xuño Lake against depth in three spatial sampling points (i.e., L1—*P. australis* area, L2—*S. lacustris* area, L3—Open waters) and in two different seasons (spring and summer 2011): F1—Fe associated with mobile and interchangeable metals; F2—Fe associated with carbonates; F3—Fe associated with iron oxides and hydroxides; and F4—Fe linked to pyrite

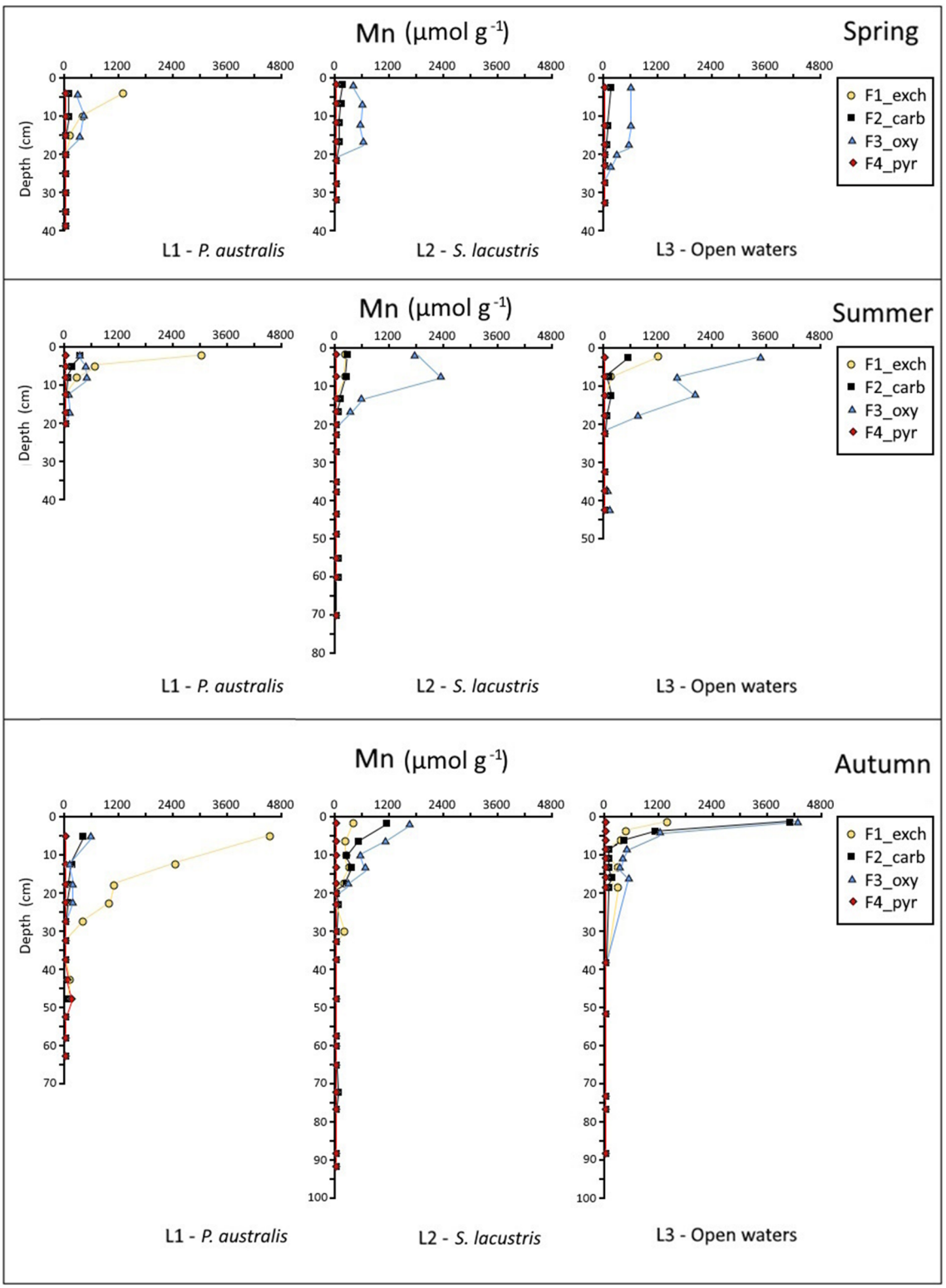


Fig. 9 Spatial and temporal variations in the contents of different Mn fractions (µmol g^{-1}) in sediment profiles from Xuño Lake against depth in three spatial sampling points (i.e., L1—*P. australis* area, L2—*S. lacustris* area, L3—open waters) and in three different seasons (spring, summer and autumn 2011): F1—Mn associated with mobile and interchangeable metals; F2—Mn associated with carbonates; F3—Mn associated with iron oxides and hydroxides; and F4—Mn linked to pyrite

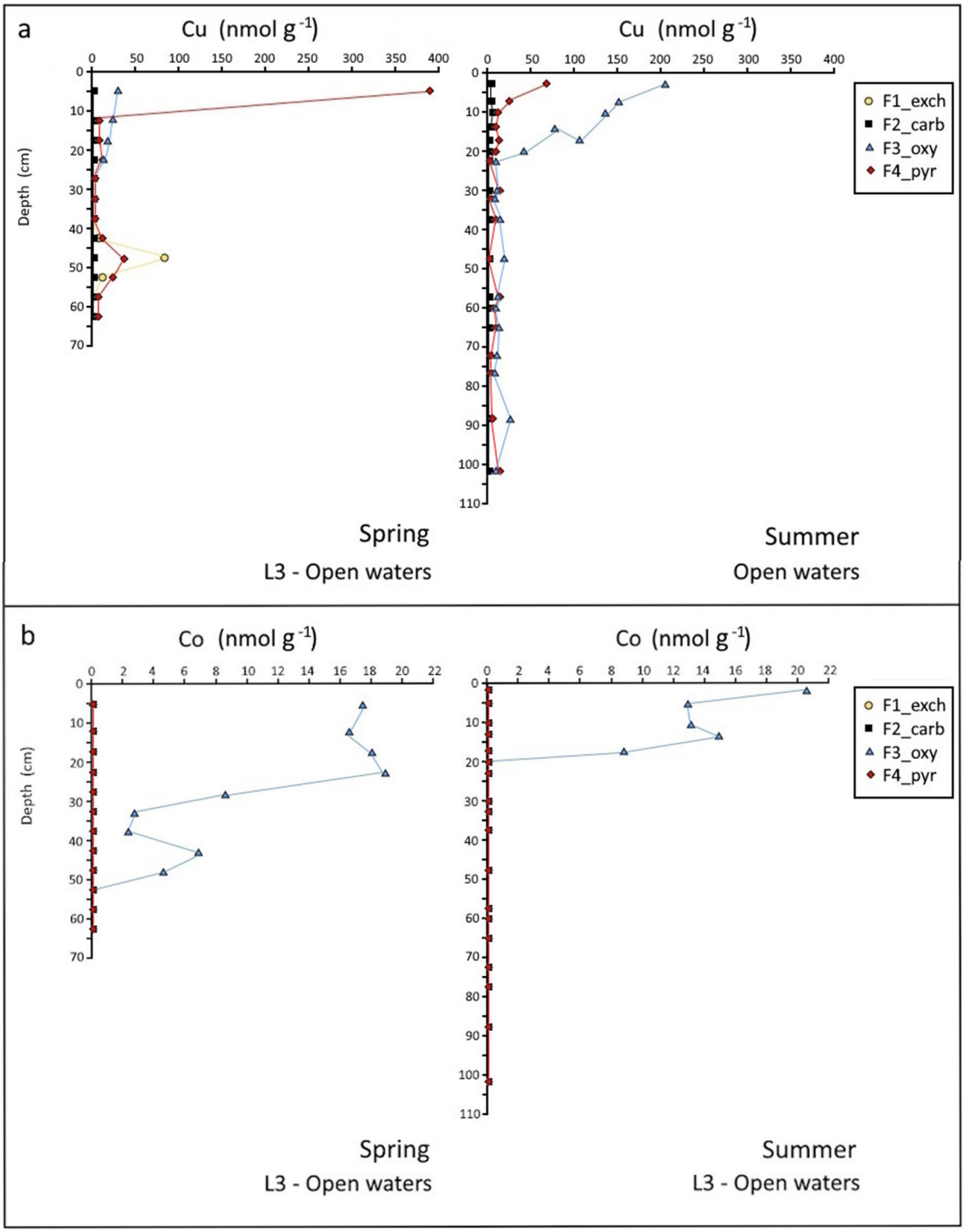


Fig. 10 Spatial and temporal variations in contents of different fractions of **a** Cu and **b** Co (nmol g^{-1}) in sediment profiles from Xuño Lake against depth in open waters (L3) and in two different seasons (spring and summer 2011): F1—Cu/Co associated with mobile and interchangeable metals; F2—Cu/Co associated with carbonates; F3—Cu/Co associated with iron oxides and hydroxides; and F4—Cu/Co linked to pyrite

However, Fe content in the oxidizable fractions (F1, F2 and F4) does not explain the 100–300 µmol g^{-1} increase observed in the F3 fraction in summer–autumn in the surface portion (Fig. 8). Therefore, we interpret the increase in Fe oxyhydroxides that occurs on the sediment surface also as a consequence of the oxidation of soluble Fe mobilized

through the water table. The high concentrations of Fe associated with fractions F1 and F2 compared with those observed in intertidal environments (Otero and Macías 2011) is consistent with the incorporation of Fe(II) into the exchange complex or its precipitation as Fe carbonate.

The drop in water level implies the greatest Fe(III) precipitation from water-soluble Fe concentrates in the deepest part of the lake in summer–autumn. Fe(II), under oxic conditions (Eh > 400 mV) and circumneutral pH (~ 7), precipitates as Fe(III) oxyhydroxide, according to reaction (1). This reaction has fast kinetics; therefore, Fe shows a more conservative behaviour in sediment than other metals, such as Mn (Otero et al. 2009; Caetano et al. 1997).

$$4\,Fe^{2+} + O_2 + 6\,H_2O \rightarrow 4\,FeOOH + 8\,H^+. \quad (1)$$

The pyritic fraction (F4) is in the minority (< 5 µmol g^{-1}), both spatially and throughout sediment depth profiles (Figs. 4d–f and 8); thus, most sulfur (S) comes from organic matter, unlike in the case of lagoons and marshes (Otero and Macías 2002, 2003). The factors limiting the formation of pyrite in sediments, according to Berner et al. (1979), are the following: (i) absence of labile organic matter available to sulfate-reducing bacteria (SRB); (ii) availability of reactive Fe (hydro-)oxides; and (iii) below-threshold sulfate concentrations in water, limiting the metabolic activity of SRBs.

The high content of organic matter (Fig. 4a–c) and Fe in sediments (Fig. 8), especially in upper levels, is not a limitation for pyrite formation. The high C:S ratio indicates that Xuño Lake is a freshwater environment with low sulfate levels due to the siliceous lithology of the watershed and the absence of marine influence (Table 1; Fig. 5). Sulfates in the lake's waters are very low throughout the year (< 25 mg l^{-1}) (Table 1); in addition, values are lower than the activity threshold for SRBs (160–288 mg kg^{-1}) in the sediment (Boudreau and Westrich 1984; Van Cappellen and Wang 1996).

Mn showed differences with Fe in terms of their geochemical dynamics in Xuño Lake (Fig. 9). Mn fractions in sediment showed differences between the zone covered by *P. australis,* dominated by F1, and the other two zones, the central zone and the zone covered by *S. lacustris*, which were dominated by F3 (Fig. 9). F1, the fraction of interchangeable or soluble Mn(II), is a mineral phase that controls the solubility of this element. The solubility of Mn(II) in non-sulfate-reducing or suboxic–anoxic environments is controlled by carbonates, either by adsorption or coprecipitation with calcite in alkaline waters (Middelburg et al. 1987; Mucci 1988; Böttcher 1998), by S in sulfide–anoxic environments (Huerta Díaz and Morse 1992; Otero and Macías 2003).

The alternation of oxic conditions throughout the year, the slightly acidic pH and the low alkalinity of water make Mn(II) the most stable geochemical form in the lake, because it remains reduced even under oxic conditions, since its oxidation kinetics are very slow, and Mn(IV) oxides and hydroxides that have a high surface area and low crystallinity are rapidly reduced by microbial activity (Stumm and Morgan 2003; Otero et al. 2009). Mn also has a low degree of pyritization in concordance with Fe: Mn pyritization becomes important at pyritization degrees higher than 50% of free Fe, since Mn sulfides are very soluble and unstable (Huerta-Díaz and Morse 1992; Otero and Macías 2002; 2003).

Copper showed differences with Fe and Mn in terms of their geochemical dynamics in Xuño Lake (Fig. 10a). F4, the Cu fraction linked to pyrite, is the dominant one, with pyritization degrees higher than 75% that can be explained by the low sulfate contents and the higher affinity of Cu for sulfides (Huerta-Díaz and Morse 1992), which displaces Fe in pyritization reaction 1.2 (Di Toro et al. 1990). The pyritization of Fe and Cu is approximately 1:1 in marine sediments; however, the low sulfate content in the freshwater Xuño Lake is the main limitation for pyrite formation (Otero et al. 2000):

$$FeS + Cu^{2+} \Leftrightarrow Fe^{2+} + CuS. \quad (2)$$

Cobalt is mainly linked to Fe oxyhydroxides (F2) (Fig. 10b), although it also forms highly stable sulfides (Huerta-Díaz and Morse 1990; 1992), but the low pyritization degree is a result of the high solubility of sulfide Co in non-oxidant acids, such as hydrofluoric acid. Thus, it could have been dissolved by chemical attacks prior to the extraction of the pyrite fraction (Morse and Luther 1999).

Comparatively, the levels of metals in the sediment have been as follows: Mn (0–4300 µmol g^{-1}) > Fe (0–600 µmol g^{-1}) > Cu (0–400 nmol g^{-1}) > Co (0–21 nmol g^{-1}) (Figs. 8, 9 and 10). The levels of Fe, Mn, Cu and Co in the vertical profile of the sedimentary record are stable below 20–25 cm depth, with the exception in spring of Co up to 55 cm depth. The dominant fraction in Fe, Mn and Co is F3 (associated with Fe oxides and hydroxides), with the exception of Mn, since the dominant one is F1 (interchangeable or soluble) in the *P. australis* vegetation zone. On the other hand, the dominant fraction in Cu is F4 (pyritic) due to its high affinity for S, although under summer anoxia conditions the majority fraction is F3.

Conclusions

The Xuño freshwater coastal shallow lake shows an eutrophic status due to its high N and P nutrient levels in the water column, although nutrient levels do not come from the basin based on the low nutrient levels in the tributary

river. Microbiological data indicate a great contribution from bird droppings in terms of nutrient input into water in relation to the lake's small dimensions. The lake's oxic conditions due to its low volume also entail high oxygenation rates in sediment, even in spite of the high evaporation rates during summer, leading to decreased water level and increased water conductivity. Depth determines the ecology of shallow lakes, which can remain well-mixed and oxygenated from surface to bottom over the summer months, while the bottom can receive a sufficient amount of sunlight to stimulate phytoplankton and aquatic macrophytes. The oxic conditions on the sediment surface limit nutrient diffusion in the water–sediment interface, especially in the case of P, which remains immobilized by Fe in the sediment, as well as of trace metals and metalloids, whose levels remain always below the contamination threshold, both in waters and in sediments. In addition, oxygen saturation regulates the levels and bioavailability of Hg in water, and the Hg concentration is even high (0.11–0.15 μg l^{-1}) under suboxic conditions (5.37–9.80 O_2 mg l^{-1}).

The levels of P and metals (i.e., Fe, Mn, Cu, and Co) are higher towards the surface of the profile, where oxic conditions keep them immobilized in the sediment. The majority fraction of the metals studied in the sediment is bound to Fe oxides and hydroxides, with the exception of the pyritic under oxic conditions for Cu and the interchangeable/soluble fraction for Mn in the *P. australis* area. The P and trace metals studied in sediment profiles are related to the highest proportion of clay fraction and organic matter in these profiles.

Top-down regulation of the water column in the Xuño shallow lake mediates the diffusion of nutrients and metals at the sediment–water interface, buffering eutrophication levels by keeping P immobilized in the sediment under oxic conditions like a nutrient pump. However, a change in water conditions can cause a release, primarily of P, and lead to a regime shift due to eutrophication, because there is no clear component or phase controlling nutrient solubility.

The cover of helophyte species *P. australis* and *S. lacustris* showed differences in the assimilation of organic monoester and diester P forms in the sediment. Therefore, due to the high biomass of macrophytes, they play a key role in P recycling within the lake. The cover of macrophyte species *P. australis* and *S. lacustris* does not determine metal dynamics in sediment profiles. However, *P. australis* determines the concentration of Mn fractions in sediment, possibly due to its high biomass compared with the other studied areas.

Author contributions X.L.O. original concept, X.L.O. and R.C. wrote the main manuscript text, X.L.O. and P.F. conducted field sampling, made chemical water and sediment analysis, drafting and editing manuscript, R.C. prepared figure 1, P.F. prepared tables 1-2 and figures 2-10, A.M. made the 31P NMR spectrum analysis in sediments. All authors reviewed the manuscript.

Funding Open Access funding provided thanks to the CRUE-CSIC agreement with Springer Nature. Open Access funding provided thanks to the University of Valencia (UVEG), trough CRUE–CSIC agreement with Springer Nature. We are grateful for grant Axudas á consolidación e estruturación de unidades de investigación competitivas do SUG do Plan Galego IDT, Ambiosol Group (ED431C-2022/40) funded by Consellería de Educación, Universidade e Formación Profesional of the autonomous government of Xunta de Galicia. Also, we are grateful for grant FJC project (FJC-2021–046415-I) of the Ministry of Science and Innovation of Spain financed by the Next Generation fund of the European Union. Rafael Carballeira is grateful for a PhD fellowship from the Xunta de Galicia (Plan I2C) and Juan de la Cierva postdoctoral contract (FJC-2021–046415-I) of the Ministry of Science and Innovation of Spain financed by the Next Generation fund of the European Union.

Declarations

Conflict of interest The authors have not disclosed any competing interests.

Open Access This article is licensed under a Creative Commons Attribution 4.0 International License, which permits use, sharing, adaptation, distribution and reproduction in any medium or format, as long as you give appropriate credit to the original author(s) and the source, provide a link to the Creative Commons licence, and indicate if changes were made. The images or other third party material in this article are included in the article's Creative Commons licence, unless indicated otherwise in a credit line to the material. If material is not included in the article's Creative Commons licence and your intended use is not permitted by statutory regulation or exceeds the permitted use, you will need to obtain permission directly from the copyright holder. To view a copy of this licence, visit http://creativecommons.org/licenses/by/4.0/.

References

Ann Y, Reddy KR, Delfino JJ (2000a) Influence of chemical amendments on phosphorous immobilization in soils from a constructed wetland. Ecol Eng 14:157–167. https://doi.org/10.1016/S0925-8574(99)00026-9

Ann Y, Reddy KR, Delfino JJ (2000b) Influence of redox potential on phosphorous solubility in chemically amended wetland organic soils. Ecol Eng 14:169–180. https://doi.org/10.1016/S0925-8574(99)00027-0

ATSDR (2004) Toxicological profile for cobalt. Agency for Toxic Substances and Disease Registry. US. Department of Health and Human Services, Atlanta, p 418

Benndorf J, Böing W, Koop J, Neubauer I (2002) Top-down control of phytoplankton: the role of time scale, lake depth and trophic state. Freshw Biol 47:2282–2295. https://doi.org/10.1046/j.1365-2427.2002.00989.x

Bernárdez P, Prego R, Filgueiras AV, Ospina-Álvarez N, Santos-Echeandía J, Álvarez-Vázquez MA, Caetano M (2017) Lithogenic sources, composition and intra-annual variability of suspended particulate matter supplied from rivers to the Northern Galician Rias (Bay of Biscay). J Sea Res 130:73–84. https://doi.org/10.1016/j.seares.2017.05.006

Berner RA (1982) Burial of organic carbon and pyrite sulfur in the modern ocean: its geochemical and environmental significance. Am J Sci 282:451–473. https://doi.org/10.2475/ajs.282.4.451

Berner RA, Raiswell R (1984) C/S method for distinguishing freshwater from marine sedimentary rocks. Geology 12:365–368. https://doi.org/10.1130/0091-7613(1984)12%3c365:CMFDFF%3e2.0.CO;2

Berner RA, Baldwin T, Holdren GR (1979) Authigenic iron sulphides as paleosalinity indicators. J Sediment Res 49:1345–1350. https://doi.org/10.1306/212F7923-2B24-11D7-8648000102C1865D

Blomqvist S, Gunnars A, Elmgren R (2004) Why the limiting nutrient differs between temperate coastal seas and freshwater lakes: a matter of salt. Limnol Oceanogr 49:2236–2241. https://doi.org/10.4319/lo.2004.49.6.2236

Böttcher ME (1998) Manganese(II) partitioning during experimental precipitation of rhodochrosite-calcite solid solutions from aqueous solutions. Mar Chem 62:287–297. https://doi.org/10.1016/S0304-4203(98)00039-5

Boudreau BP, Westrich JT (1984) The dependence of bacterial sulfate reduction on sulfate concentration in marine sediments. Geochim Cosmochim Acta 48:2503–2516. https://doi.org/10.1016/0016-7037(84)90301-6

Branfireun BA, Cosio C, Poulain AJ, Riise G, Bravo AG (2020) Mercury cycling in freshwater systems—an updated conceptual model. Sci Total Environ 745:140906. https://doi.org/10.1016/j.scitotenv.2020.140906

Bruland KW, Franks R, Knauer GA, Martin JH (1979) Sampling and analytical methods for the determination of copper, cadmium, zinc, and nickel at the nanogram per liter in sea water. Mar Chem 105:233–245. https://doi.org/10.1016/S0003-2670(01)83754-5

Cade-Menun BJ (2005) Using phosphorus 31 nuclear magnetic resonance spectroscopy to characterize organic phosphorus in environmental samples. In: Turner BL, Frossard E, Baldwin DS (eds) Organic phosphorus in the environment. CABI Publishing, Wallingford, pp 21–44

Caetano M, Falçao M, Vale C, Bebianno MJ (1997) Tidal flushing of ammonium, iron and manganese from inter-tidal sediment pore water. Mar Chem 58:203–211. https://doi.org/10.1016/S0304-4203(97)00035-2

Carey C, Rydin E (2021) Lake trophic status can be determined by the depth distribution of sediment phosphorus. Limnol Oceanogr 56(6):2051–2063. https://doi.org/10.4319/lo.2011.56.6.2051

Carrillo V, Collins C, Brisson J, Vidal G (2021) Evaluation of long-term phosphorus uptake by *Schoenoplectus californicus* and *Phragmites australis* plants in pilot-scale constructed wetlands. Int J Phytoremediation 24(6):610–621. https://doi.org/10.1080/15226514.2021.1960478

D'Itri FM (1972) The environmental mercury problem, 1st edn. CRC Press. The Chemical Rubber Company, Cleveland, p 142

Declerck S, Vandekerkhove J, Johansson L, Muylaert K, Conde-Porcuna JM, Van der Gucht K, Pérez-Martínez C, Lauridsen T, Schwenk K, Zwart G, Rommens W, López-Ramos J, Jeppesen E, Vyverman W, Brendonck L, De Meester L (2005) Multi-group biodiversity in shallow lakes along gradients of phosphorus and water plant cover. Ecol 86(7):1910–1915. https://doi.org/10.1890/04-0373

Decree 37/2014 (2014) Declaration of special conservation zones the places of community importance in Galicia and the approval of the Master Plan of the Natura 2000 Network of Galicia. Diario Oficial de Galicia 62, 31 March 2014, pp. 13427–13888. (https://www.xunta.gal/dog/Publicados/2014/20140331/AnuncioCA02-270314-0001_gl.pdf) (**in Galician**). Accessed 25 July 2023

Dejoux C (1983) The impact of birds on the lacustrine ecosystem. In: Carmouze JP, Durand JR, Lévêque C (eds) Lake Chad Monographiae. Biologicae 53. Springer, Dordrecht, pp 519–526. https://doi.org/10.1007/978-94-009-7266-7_17

Di Toro DM, Mahony JD, Hansen DJ, Scott KT, Hiks MB, Mayr SM, Redmont MS (1990) Toxicity of Cd in sediments: the role of acid volatile sulphide. Envir Toxicol Chem 9:1489–1504. https://doi.org/10.1002/etc.5620091208

Dolman AM, Mishcke UM, Wiedner C (2016) Lake-type-specific seasonal patterns of nutrient limitation in German lakes, with target nitrogen and phosphorus concentrations for good ecological status. Freshw Biol 61(4):444–456. https://doi.org/10.1111/fwb.12718

Duval B, Tessier E, Kortazar L, Fernandez LA, de Diego A, Amouroux D (2023) Dynamics, distribution, and transformations of mercury species from pyrenean high-altitude lakes. Environ Res 216(2):114611. https://doi.org/10.1016/j.envres.2022.114611

European Directive (92/43/CE) European Parliament and the council of 22 July 1992 on the conservation of natural habitats and of wild fauna and flora. Official Journal of the European Union L 206, 22 July 1992, pp. 7–50. https://eur-lex.europa.eu/legal-content/EN/TXT/PDF/?uri=CELEX:31992L0043. Accessed 25 July 2023

European Union Directive (2006/7/EC) European Parliament and the council of 15 February 2006 concerning the management of bathing water quality and repealing Directive 76/160/EEC. Official Journal of the European Union L 64, 15 February 2006, pp. 37–51. https://eur-lex.europa.eu/legal-content/EN/TXT/?uri=celex%3A32006L0007. Accessed 25 July 2023

Fernández-Gómez C, Bayona JM, Díez S (2012) Laboratory and field evaluation of diffusive gradient in thin films (DGT) for monitoring levels of dissolved mercury in natural river water. Int J Environ Anal Chem 92:1689–1698. https://doi.org/10.1080/03067319.2011.581369

Foley B, Jones ID, Maberly SC, Rippey B (2012) Long-term changes in oxygen depletion in a small temperate lake: effects of climate change and eutrophication. Freshwat Biol 57:278–289. https://doi.org/10.1111/j.1365-2427.2011.02662.x

Fortin D, Leppard GG, Tessier A (1993) Characteristic of lacustrine diagenetic iron oxyhydroxides. Geochim Cosmochim Acta 57:4391–4404. https://doi.org/10.1016/0016-7037(93)90490-N

Fraga-Santiago P, Gómez-Pazo A, Pérez-Alberti A, Montero P, Otero-Pérez XL (2019) Trends in the recent evolution of Coastal Lagoons and Lakes in Galicia (NW Iberian Peninsula). J Mar Sci Eng 7(8):272. https://doi.org/10.3390/jmse7080272

Free G, Tierney D, Little R, Kelly FL, Kennedy B, Plant C, Trodd W, Wynne C, Caroni R, Byrne C (2016) Lake ecological assessment metrics in Ireland: relationships with phosphorous and typology parameters and the implications for setting nutrient standards. Biol Environ 116(3):191–204. https://doi.org/10.1353/bae.2016.0015

Gaget E, Le Viol I, Pavón-Jordán D, Cazalis V, Kerbiriou C, Jiguet F, Popoff N, Dami L, Mondain-Monval JY, du Rau PD, Abdou WAI, Bozic L, Dakki L, Encarnação VMF, Erciyas-Yavuz K, Etayeb KS, Molina B, Petkov N, Uzunova D, Zenatello M, Galewski T (2020) Assessing the effectiveness of the Ramsar Convention in preserving wintering waterbirds in the Mediterranean. Biol Conserv 243:108485. https://doi.org/10.1016/j.biocon.2020.108485

García-Oliva F, Merino A, Fonturbel M, Omil B, Fernández C, Vega JA (2018) Severe wildfire hinders renewal of soil P pools by thermal mineralization of organic P in forest soil: analysis by sequential extraction and ^{31}P NMR spectroscopy. Geoderma 309:32–40. https://doi.org/10.1016/j.geoderma.2017.09.002

Gebremariam SY, McCormick P, Rochelle P (2021) Evidence of a rapid phosphorus-induced regime shift in a large deep reservoir. Sci Total Environ 782:146755. https://doi.org/10.1016/j.scitotenv.2021.146755

Gere G, Andrikovics S (1992) Effects of waterfowl on water quality. Hydrobiologia 243:445–448. https://doi.org/10.1007/BF00007061

Gu B, Bian Y, Miller CL, Dong W, Jiang X, Liang L (2011) Mercury reduction and complexation by natural organic matter in anoxic environments. PNAS 108(4):1479–1483. https://doi.org/10.1073/pnas.1008747108

Hansen HP, Koroleff F (1999) Determination of nutrients. In: Grasshoff K, Kremling K, Ehrhardt M (eds) Methods of seawater analysis. Wiley-VCH Verlag, Weinheim, pp 159–226

Hansson LA, Nicolle A, Brönmark C, Hargeby A, Lindström A, Andersson G (2010) Waterfowl, macrophytes, and the clear water state of shallow lakes. Hydrobiologia 646:101–109. https://doi.org/10.1007/s10750-010-0169-z

Harrault L, Allard B, Mériguet J, Carmignac D, Huon S, Gauzens B, Lacroix G (2014) Bottom-up effects of lake sediment on pelagic food-web compartments: a mesocosm study. Freshw Biol 59(8):1695–1709. https://doi.org/10.1111/fwb.12375

Hickey CH, Gibbs MM (2009) Lake sediment phosphorus release management—decision support and risk assessment framework. N Z J Mar Freshw Res 43(3):819–856. https://doi.org/10.1080/00288330909510043

Hogan DM, Jordan TE, Walbridge MR (2004) Phosphorus retention and soil organic carbon in restored and natural freshwater wetlands. Wetlands 24:573–585. https://doi.org/10.1672/0277-5212(2004)024[0573:PRASOC]2.0.CO;2

Holmboe N, Kristensen E, Andersen FO (2001) Anoxic decomposition in sediments from a tropical mangrove forest and temperate Wadden Sea: implications of N and P addition experiments. Estuar Coast Shelf Sci 53:125–140. https://doi.org/10.1006/ecss.2000.0794

Hsu-Kim H, Kucharzyk KH, Zhang T, Deshusses MA (2013) Mechanisms regulating mercury bioavailability for methylating microorganisms in the aquatic environment: a critical review. Environ Sci Technol 47(6):2441–2456. https://doi.org/10.1021/es304370g

Huerta-Díaz MA, Morse JW (1990) A quantitative method for determination of trace metal concentrations in sedimentary pyrite. Mar Chem 29:119–144. https://doi.org/10.1016/0304-4203(90)90009-2

Huerta-Díaz MA, Morse JW (1992) Pyritization of trace metals in anoxic marine sediments. Geochim Cosmochim Acta 56:2681–2702. https://doi.org/10.1016/0016-7037(92)90353-K

Huerta-Díaz MA, Tessier A, Carignan R (1998) Geochemistry of trace metals associated with reduced sulfur in freshwater sediments. Appl Geochemistry 13(2):213–233. https://doi.org/10.1016/S0883-2927(97)00060-7

Hupfer M, Dollan A (2003) Immobilisation of phosphorus by iron-coated roots of submerged macrophytes. Hydrobiologia 506–509:635–640. https://doi.org/10.1023/B:HYDR.0000008605.09957.07

IGME (1981) Sheet 151 (3–9)–Puebla de Caramiñal. MAGNA 50 - Geological Map of Spain at a scale of 1:50,000 (2nd Series) (**in Spanish**)

Janse JH, De Senerpont Domis LN, Scheffer M, Lijklema L, Van Liere L, Klinge M, Mooij WM (2008) Critical phosphorus loading of different types of shallow lakes and the consequences for management estimated with the ecosystem model PCLake. Limnologica 38(3–4):203–219. https://doi.org/10.1016/j.limno.2008.06.001

Janssen ABG, Hilt S, Kosten S, de Klein JJM, Paerl HW, Van de Waal DB (2021) Shifting states, shifting services: Linking regime shifts to changes in ecosystem services of shallow lakes. Freshw Biol 66(1):1–12. https://doi.org/10.1111/fwb.13582

Jeppesen E, Jensen JP, Søndergaard M, Lauridsen T, Pedersen LJ, Jensen L (1997) Top-down control in freshwater lakes: the role of nutrient state, submerged macrophytes and water depth. Hydrobiologia 342:151–164. https://doi.org/10.1023/A:1017046130329

Jeppesen E, Meerhoff M, Davidson TA, Trolle D, Søndergaard M, Lauridsen TL, Beklioglu M, Brucet S, Volta P, González-Bergonzoni V, Nielsen A (2014) Climate Change Impacts on Lakes: An Integrated Ecological Perspective Based on a Multi-Faceted Approach, With Special Focus on Shallow Lakes. J Limnol 73(s1):88–111. https://doi.org/10.4081/jlimnol.2014.844

Jiménez-Cárceles FJ, Álvarez-Rogel J (2008) Phosphorus fractionation and distribution in a salt marsh soils affected by mine wastes and eutrophicated water: a case study in SE Spain. Geoderma 144:299–309. https://doi.org/10.1016/j.geoderma.2007.11.024

Jiménez-Cárceles FJ, Álvarez-Rogel J, Egea-Nicolás C, González-Alcaraz MN, Cervantes AM, Conesa-Alcaraz HM (2011) The role of salt marshes in reducing the concentration of nitrate and phosphorus in eutrophicated water: the Mar Menor Lagoon, a case study in Semiarid Mediterranean areas of SE Spain. In: Otero XL, Macías F (eds) Biogeochemistry and pedogenetic process in saltmarsh and mangrove systems. Noca Science Publishers, New York, pp 205–232 (**ISBN: 9781617282690**)

Joshi SR, Kukkadapu RK, Burdige DJ, Bowden ME, Sparks DL, Jaisi DP (2015) Organic matter remineralization predominates phosphorus cycling in the mid-bay sediments in the Chesapeake Bay. Environ Sci Technol 49(10):5887–5896. https://doi.org/10.1021/es5059617

Kim LH, Choi E, Stenstrom MK (2003) Sediment characteristics, phosphorus types and phosphorus release rates between river and lake sediments. Chemosphere 50(1):53–61. https://doi.org/10.1016/S0045-6535(02)00310-7

Kleijn D, Cherkaoui I, Goedhart PW, van der Hout J, Lammertsma D (2014) Waterbirds increase more rapidly in Ramsar designated wetlands than in unprotected wetlands. J Appl Ecol 51:289–298. https://doi.org/10.1111/1365-2664.12193

Labry C, Herbland A, Delmas H (2002) The role of phosphorus on planktonic production of the Gironde plume waters in the Bay of Biscay. J Plankton Res 24:97–117. https://doi.org/10.1093/plankt/24.2.97

Lau MP, Del Giorgio P (2020) Reactivity, fate and functional roles of dissolved organic matter in anoxic inland waters. Biol Lett 16(2):20190694. https://doi.org/10.1098/rsbl.2019.0694

Leventhal JS (1995) Carbon-sulfur plots to show diagenetic and epigenetic sufidation in sediments. Geochim Cosmochim Acta 59(6):1207–1211. https://doi.org/10.1016/0016-7037(95)00036-Y

Li H, Song C, Yang L, Qin H, Cao X, Zhou Y (2021) Phosphorus supply pathways and mechanisms in shallow lakes with different regime. Water Res 193:116886. https://doi.org/10.1016/j.watres.2021.116886

Ligeza S, Smal H (2003) Accumulation of nutrients in soils affected by perennial colonies of piscivorous birds with reference to biogeochemical cycles of elements. Chemosphere 52:595–602. https://doi.org/10.1016/S0045-6535(03)00241-8

Maberly SC, O'Donnell RA, Woolway RI, Cutler MEJ, Gong M, Jones ID, Merchant CJ, Miller CA, Politi E, Scott EM, Thackeray SJ, Tyler AN (2020) Global lake thermal regions shift under climate change. Nat Commun 11:1232. https://doi.org/10.1038/s41467-020-15108-z

Membiela P, Montes C, Martínez-Ansemil E (1991) Características hidroquímicas de los ríos de Galicia (NW Peninsula Ibérica). Limnetica 7:163–174

Middelburg JJ, De Lange GJ, van der Weijden CH (1987) Manganese solubility control in marine pore waters. Geochim Cosmochim Acta 51:759–763. https://doi.org/10.1016/0016-7037(87)90086-X

Morse JW, Luther GW (1999) Chemical influences on trace metal-sulfide interactions in anoxic sediments. Geochim Cosmochim

Acta 63:3373–3378. https://doi.org/10.1016/S0016-7037(99)00258-6

Moss B, Beklioglu M, Carvalho L, Kilinc S, McGowan S, Stephen D (1997) Vertically-challenged limnology; contrasts between deep and shallow lakes. Hydrobiologia 342:257–267. https://doi.org/10.1023/A:1017059928028

Mucci A (1988) Manganese uptake during calcite precipitation from seawater: conditions leading to the formation of a pseudokutnahorite. Geochim Cosmochim Acta 52:1859–1868. https://doi.org/10.1016/0016-7037(88)90009-9

Nag R, Cummins E (2021) Analysis of the levels of metal(loid)s in environmental compartments in Ireland towards a screening measure for potential relative risk using open-source datasets. J Environ Manage 298:113531. https://doi.org/10.1016/j.jenvman.2021.113531

Noack SR, McLaughlin MJ, Smernik RJ, McBeath TM, Armstrong RD (2012) Crop residue phosphorus: speciation and potential bioavailability. Plant Soil 359:375–385. https://doi.org/10.1007/s11104-012-1216-5

Nóbrega GN, Otero XL, Macías F, Ferreira T (2014) Phosphorus geochemistry in a Brazilian semiarid mangrove soil affected by shrimp farm effluents. Environ Monit Assess 186:5749–5762. https://doi.org/10.1007/s10661-014-3817-3

Nowlin WH, Evarts JL, Vanni MJ (2005) Release rates and potential fates of nitrogen and phosphorus from sediments in a eutrophic reservoir. Freshw Biol 50(2):301–322. https://doi.org/10.1111/j.1365-2427.2004.01316.x

Otero XL, Fernández-Sanjurjo MJ (1999) Seasonal Variation in inorganic nitrogen content of soils from breeding sites of yellow-legged gulls (*Larus cachinnans*) in the Cíes Island Natural Park (NW Iberian Peninsula). Fresenius Environ Bull 8:685–692

Otero XL, Macías F (2002) Variation with depth and season in metal sulfides in salt marsh soils. Biogeochemistry 61:247–268. https://doi.org/10.1023/A:1020230213864

Otero XL, Macías F (2003) Spatial variation in pyritization of trace metals in salt-marsh soils. Biogeochemistry 62:59–86. https://doi.org/10.1023/A:1021115211165

Otero XL, Macías F (2011) Biogeochemistry and pedogenetic process in saltmarsh and mangrove systems. Nova Science Publisher, New York (**9781617282690**)

Otero XL, Sánchez JM, Macías F (2000) Bioaccumulation of heavy metals in thionic fluvisols by a marine polychaete (*Nereis diversicolor*): the role of metal sulfide. J Environ Qual 29:1133–1141. https://doi.org/10.2134/jeq2000.00472425002900040014x

Otero XL, Vidal-Torrado P, Calvo de Anta R, Macías F (2005) Trace elements in biodeposits and sediments from mussell culture in the Ría de Arousa (Galicia-NW Spain). Environ Pollut 136:119–134. https://doi.org/10.1016/j.envpol.2004.11.026

Otero XL, Ferreira TO, Huerta-Díaz MA, Partiti CSM, Souza JV, Vidal-Torrado P, Macías F (2009) Geochemistry of iron and manganese in soils and sediments of a mangrove system, Island of Pai Matos (Cananeia-SP, Brazil). Geoderma 148:318–335. https://doi.org/10.1016/j.geoderma.2008.10.016

Otero XL, Guevara P, Sánchez M, López I, Queiroz HM, Ferrera A, Ferreira TO, Nóbrega TN, Carballo R (2023) Pyrites in a salt marsh-ria system: Quantification, morphology, and mobilization. Mar Geol 455:106954. https://doi.org/10.1016/j.margeo.2022.106954

Paludan C, Jensen HS (1995) Sequential extraction of phosphorus in freshwater wetland and lake sediments: significance of humic acids. Wetlands 15:365–373. https://doi.org/10.1007/BF03160891

Paludan C, Morris JT (1999) Distribution and speciation of phosphorus along a salinity gradient in intertidal marsh sediments. Biogeochemistry 45:197–221. https://doi.org/10.1007/BF01106781

Peña-Lastra SDL, Torre F, Carballeira R, Santiso M, Pérez-Alberti A, Otero XL (2022) The Rapid Effects of Yellow-Legged Gull (*Larus michahellis*) Colony on Dune Habitats and Plant Landscape in the Atlantic Islands National Park (NW Spain). Land 11(2):258. https://doi.org/10.3390/land11020258

Poikane S, Kelly MG, Salas Herrero F, Pitt JA, Jarvie HP, Claussen U, Leujak W, Solheim AL, Teixeira H, Phillips G (2019) Nutrient criteria for surface waters under the European Water Framework Directive: Current state-of-the-art, challenges and future outlook. Sci Total Environ 695(10):133888. https://doi.org/10.1016/j.scitotenv.2019.133888

Royal Decree 817/2015. Decree establishing the criteria for monitoring and evaluating the state of surface waters and environmental quality standards. Boletín Oficial del Estado 219, 12 September 2015. https://www.boe.es/buscar/doc.php?id=BOE-A-2015-9806 (**In Spanish**)

Sáez A, Carballeira R, Pueyo JJ, Vázquez-Loureiro D, Leira M, Hernández A, Valero-Garcés BI, Bao R (2018) Formation and evolution of back-barrier perched lakes in rocky coasts: an example of a Holocene system in north-west Spain. Sedimentology 65(6):1891–1917. https://doi.org/10.1111/sed.12451

Scheffer M, van Nes EH (2007) Shallow lakes theory revisited: various alternative regimes driven by climate, nutrients, depth and lake size. Hydrobiologia 584:455–466. https://doi.org/10.1007/s10750-007-0616-7

Schlichting A, Leinweber P, Meissner R, Altermann M (2002) Sequentially extracted phosphorous fractions in peat-derived soils. J Plant Nutr Soil Sci 165:290–298. https://doi.org/10.1002/1522-2624(200206)165:3%3c290::AID-JPLN290%3e3.0.CO;2-A

Sierra J, Roig N, Giménez Papiol G, Pérez-Gallego E, Schuhmacher M (2017) Prediction of the bioavailability of potentially toxic elements in freshwaters. Comparison between speciation models and passive samplers. Sci Total Environ 605–606:211–218. https://doi.org/10.1016/j.scitotenv.2017.06.136

Sinistro R (2010) Top-down and bottom-up regulation of planktonic communities in a warm temperate wetland. J Plankton Res 32(2):209–220. https://doi.org/10.1093/plankt/fbp114

Smedley PL, Kinniburgh DG (2017) Molybdenum in natural waters: a review of occurrence, distributions and controls. Appl Geochem 84:387–432. https://doi.org/10.1016/j.apgeochem.2017.05.008

Sobek S, Durisch-Kaiser E, Zurbrügg R, Wongfun N, Wessels M, Pasche N, Wehrli B (2009) Organic carbon burial efficiency in lake sediments controlled by oxygen exposure time and sediment source. Limnol Oceanogr 54:2243–2254. https://doi.org/10.4319/lo.2009.54.6.2243

Søndergaard M, Jensen JP, Jeppesen E (2003) Role of sediment and internal loading of phosphorus in shallow lakes. Hydrobiologia 506:135–145. https://doi.org/10.1023/B:HYDR.0000008611.12704.dd

Stumm W, Morgan JJ (2003) Aquatic Chemistry. John Wiley and Sons, New York (**978-0-471-51185-4**)

Suter W (1994) Overwintering waterfowl on Swiss lakes - how are abundance and species richness influenced by trophic status and lake morphology? Hydrobiologia 279(1–14):1994. https://doi.org/10.1007/bf00027836

Tessier A, Campbell PGC, Bisson M (1979) Sequential extraction procedure for the speciation of particulate trace metals. Anal Chem 51:844–855. https://doi.org/10.1021/ac50043a017

The Venice System for the Classification of Marine Waters According to Salinity (1959) The final resolution of the symposium on the classification of brackish waters. Archiv Oceanogr Limnol 11(suppl):243–248. https://doi.org/10.4319/lo.1958.3.3.0346

Toet S, Bouwman M, Cevaall A, Verhoeven J (2005) Nutrient removal through autumn harvest of Phragmites australis and Typha latifolia shoots in relation to nutrient loading in a wetland system used for polishing sewage treatment plant effluent. J Environ

Sci Health A Toxicol Hazard Subst Environ Eng 40(6–7):1133–1156. https://doi.org/10.1081/ese-200055616

Tu L, Jarosch KA, Schneider T, Grosjean M (2019) Phosphorus fractions in sediments and their relevance for historical lake eutrophication in the Ponte Tresa basin (Lake Lugano, Switzerland) since 1959. Sci Total Environ 685:806–817. https://doi.org/10.1016/j.scitotenv.2019.06.243

Turner BL, Newman S (2005) Phosphorus cycling in wetland soils: the importance of phosphate diesters. J Environ Qual 34:1921–1929. https://doi.org/10.2134/jeq2005.0060

Turner BL, Mahieu N, Condron LM (2003) Phosphorus-31 nuclear magnetic resonance spectral assignments of phosphorus compounds in soil NaOH-EDTA extracts. Soil Sci Soc Am J 67:497–510. https://doi.org/10.2136/sssaj2003.4970

Vadeboncoeur Y, Lodge DM, Carpenter SR (2001) Whole-lake fertilization effects on the distribution of primary production between benthic and pelagic habitats. Ecol 82(4):1065–1077. https://doi.org/10.1890/0012-9658(2001)082[1065:WLFEOD]2.0.CO;2

Van Cappellen P, Wang Y (1996) Cycling of iron and manganese in surface sediments. A general theory for carbon, oxygen, nitrogen, sulfur, iron, and manganese. Am J Sci 296:197–243. https://doi.org/10.2475/ajs.296.3.197

Willby N, Pitt JA, Phillips G (2012) The ecological classification of UK lakes using aquatic macrophytes. Report-SC010080/R2. Environment Agency, Bristol.

Woolway RI, Sharma S, Weyhenmeyer GA, Sharma S, Weyhenmeyer GA, Debolskiy A, Golub M, Mercado-Bettín D, Perroud M, Stepanenko V, Tan Z, Grant L, Ladwig R, Mesman J, Moore TN, Shatwell T, Vanderkelen I, Austin JA, DeGasperi CL, Dokulil M, La Fuente S, Mackay EB, Schladow SG, Watanabe S, Marcé R, Pierson DC, Thiery W, Jennings E (2021) Phenological shifts in lake stratification under climate change. Nat Commun 12:2318. https://doi.org/10.1038/s41467-021-22657-4

Yankova Y, Neuenschwander S, Köster O, Posch T (2017) Abrupt stop of deep water turnover with lake warming: drastic consequences for algal primary producers. Sci Rep 3:13770. https://doi.org/10.1038/s41598-017-13159-9

Yu W, Yang H, Chen J, Liao P, Chen Q, Yang Y, Liu Y (2022) Organic phosphorus mineralization dominates the release of internal phosphorus in a Macrophyte-dominated eutrophication lake. Front Environ Sci 9:812834. https://doi.org/10.3389/fenvs.2021.812834

Zhang Y, Jia Q, Prins HHT, Cao HL, de Boer WF (2015) Effect of conservation efforts and ecological variables on waterbird population sizes in wetlands of the Yangtze River. Sci Rep 5:17136. https://doi.org/10.1038/srep17136

Zhu MY, Zhu GW, Zhao L, Yao X, Zhang Y, Gao G, Qin B (2013) Influence of algal bloom degradation on nutrients release at the sediment-water interface in Lake Taihu, China. Environ Sci Pollut Res 20(3):1803–1811. https://doi.org/10.1007/s11356-012-1084-9

Publisher's Note Springer Nature remains neutral with regard to jurisdictional claims in published maps and institutional affiliations.